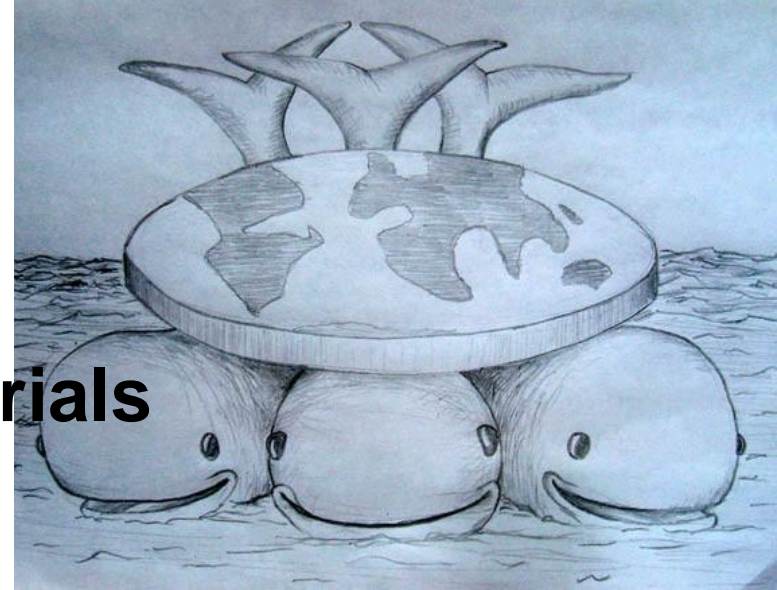


Co-proposers of SC

- **Michel Kenzelmann, Uwe Filges, PSI**
- **Yixi Su, Jörg Voigt, JCNS**
- **Andrew Sazonov, Aachen Tech**
- **University**
- **Beatrice Gillon, Isabelle Mirebeau, Alexandre Bataille, Philippe Bourges, LLB**
- **Fabienne Duc, Paul Frings, LNCMI-Toulouse**
- **Virginie Simonet , Institut Neel**
- **Josep Nogués Sanmiquel, Univ. Aut. Barcelona**
- **Igor Golosovsky, PNPI**

OUTLINE

- **Functional magnetic materials**
 - Epitaxial single crystals
 - Non-collinear Magnetism
 - Molecular Magnetism
 - Photo-crystallography
- **Emergent Phenomena and Topological States**
 - Frustrated magnets
 - Multipolar interactions
- **The challenges of superconductivity**
- **High field magnetism**
- **Electromagnon and hybrid excitations**



OUTLINE

- **Emergent Phenomena and Topological States**
- **Functional magnetic materials**
- **Non-collinear Magnetism**
- **The challenges of superconductivity**
- **Frustrated magnets**
- **Molecular Magnetism**
- **Epitaxial single crystals**
- **High field magnetism**
- **Electromagnon and hybrid excitations**

- **Functional magnetic materials**
 - **Permanent Magnets, Magneto-caloric, Magnetostrictive**
 - **Magnetic shape memory**
 - **Multiferroics (Magnetoelectrics)**
 - **Epitaxial magnets**
 - **Molecular magnets**
 - **Nano magnets**

● Functional magnetic materials

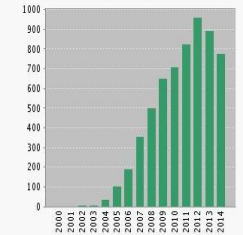
● Multiferroics (Magnetolectrics)

● Epitaxial magnetic (crystal)

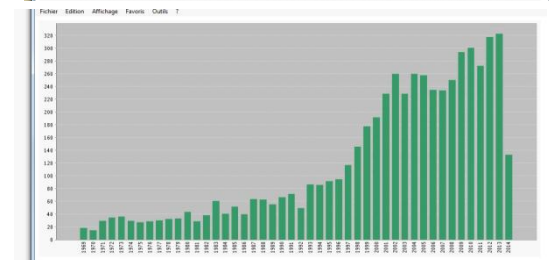
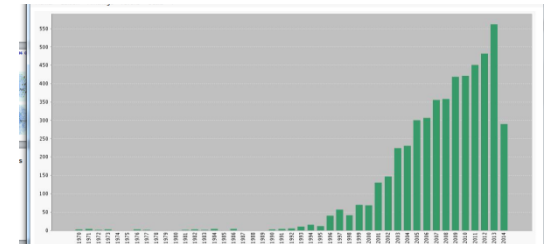
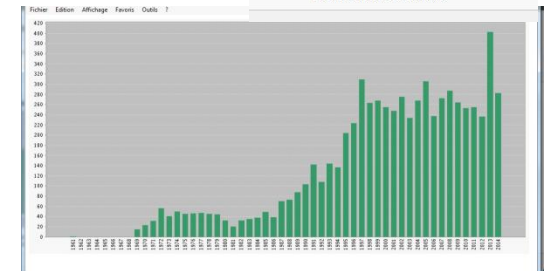
● Nano magnetic (crystal)

● Molecular magnetic (crystal)

Published Items in Each Year



The latest 20 years are displayed.



● Multiferroics (Magnetolectrics)

● TbMnO₃

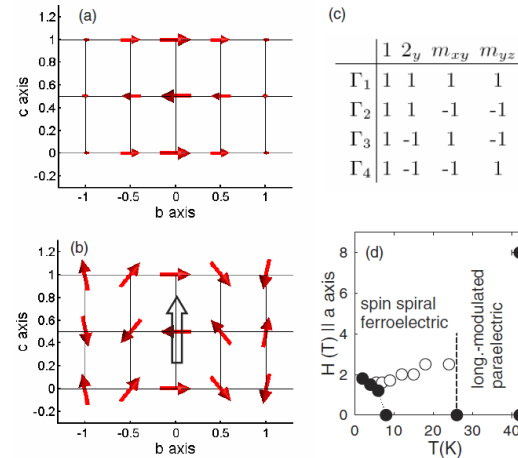
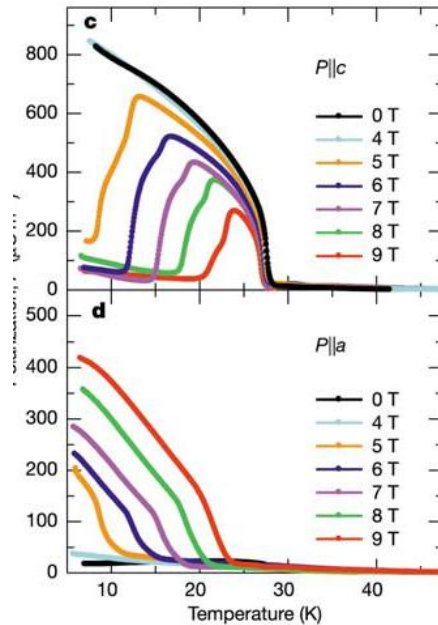
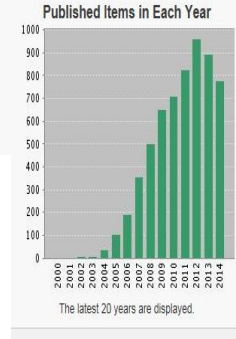


FIG. 4 (color online). Schematic of the magnetic structure at (a) $T = 35$ K and (b) $T = 15$ K, projected onto the b - c plane.



T. Kimura et al. *Nature* 426, 55, 2003

M. Kenzelmann et al., PRL 95, 087206, 2005

● **Proper FE** **Polarization** due to **Structural instability** -

● **Improper FE** **Polarization** due to some other ordering

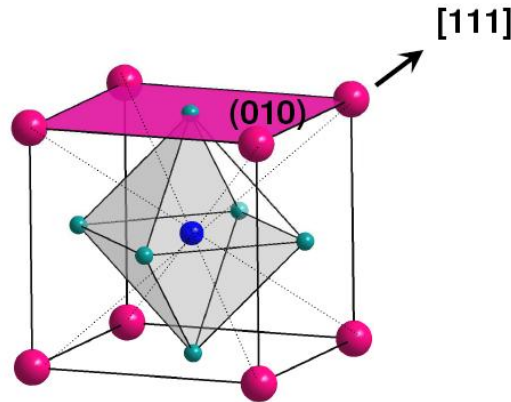
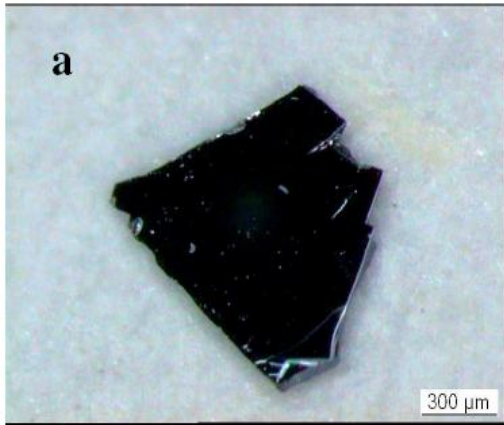
Electric-Field-Induced Spin Flop in BiFeO₃ Single Crystals at Room Temperature

D. Lebeugle,¹ D. Colson,¹ A. Forget,¹ M. Viret,¹ A. M. Bataille,² and A. Gukasov²

¹Etat Condensé, DSM/IRAMIS, CEA Saclay, F-91191 Gif-Sur-Yvette, France

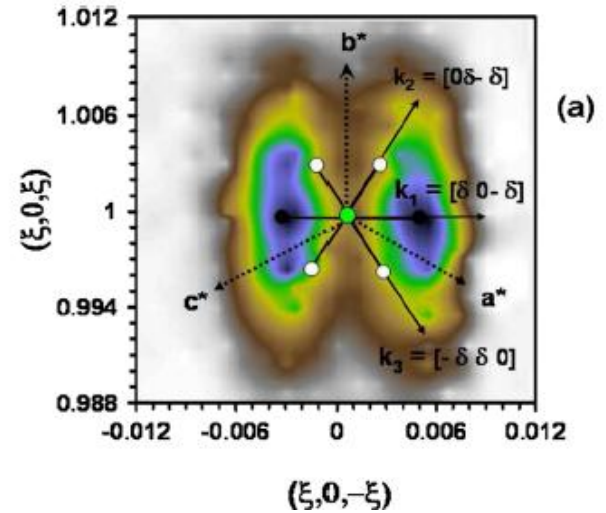
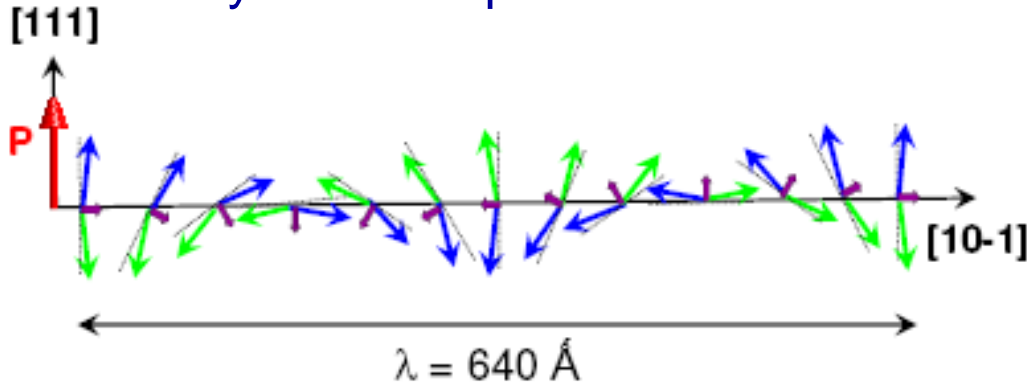
²ILL, DSM/IRAMIS, CEA Saclay, F-91191 Gif-Sur-Yvette, France

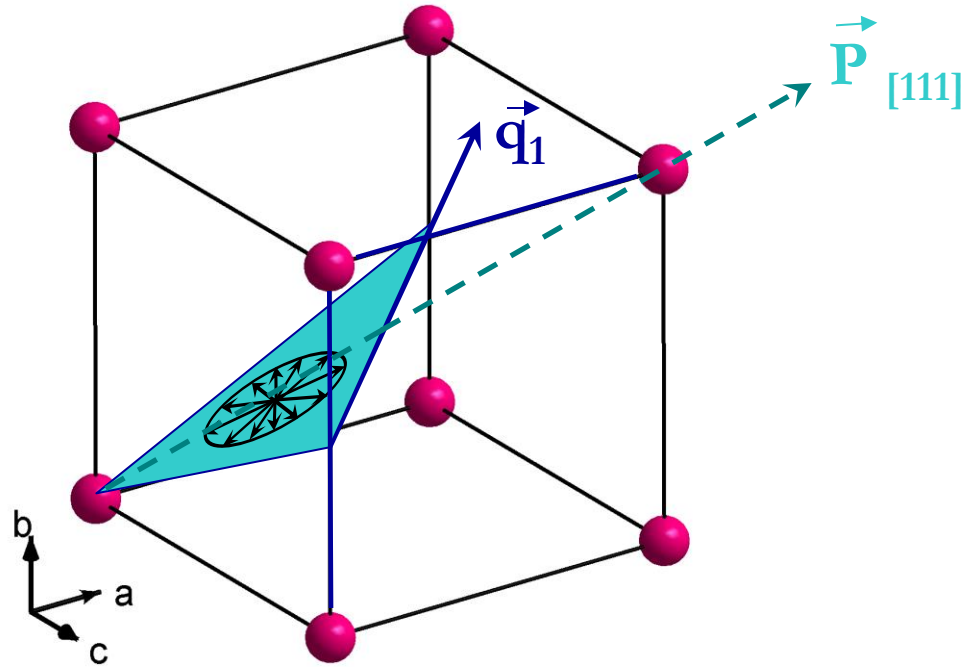
received 24 January 2008; published 2 June 2008



Etat vierge

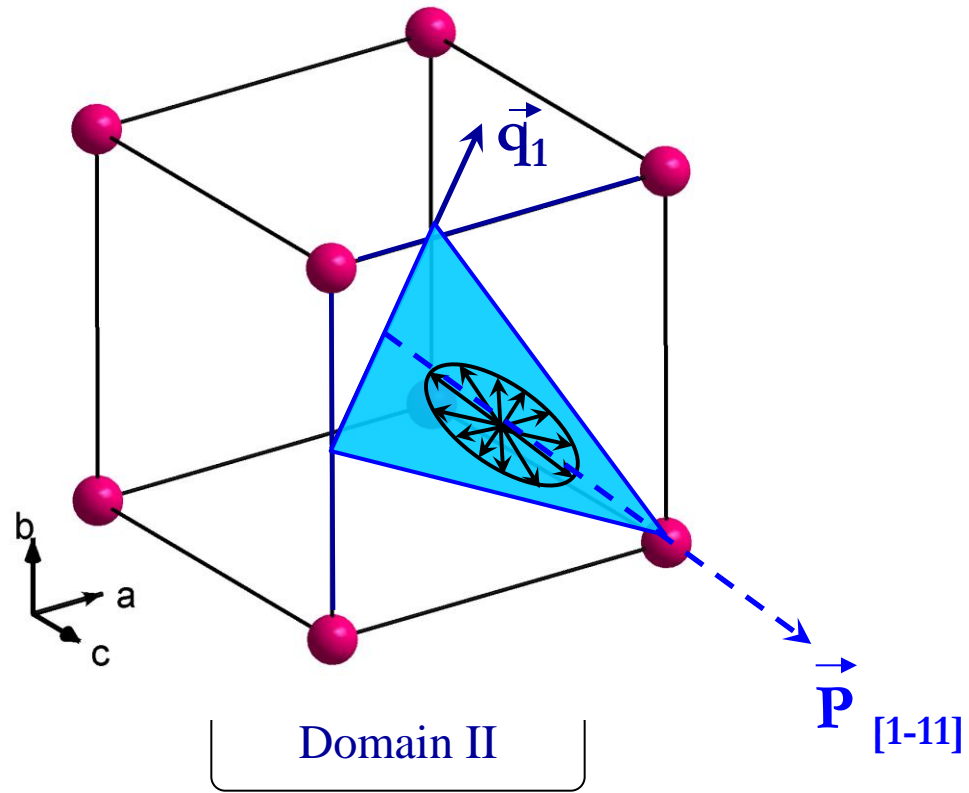
BiFeO₃, 900x800x40 μm³
Cycloïde de période 640 Å





Domain I

Rotation plane : $(-12-1) = P_{[111]} \times q_1$



Rotation plane : $(121) = P'_{[1-11]} \times q_1$

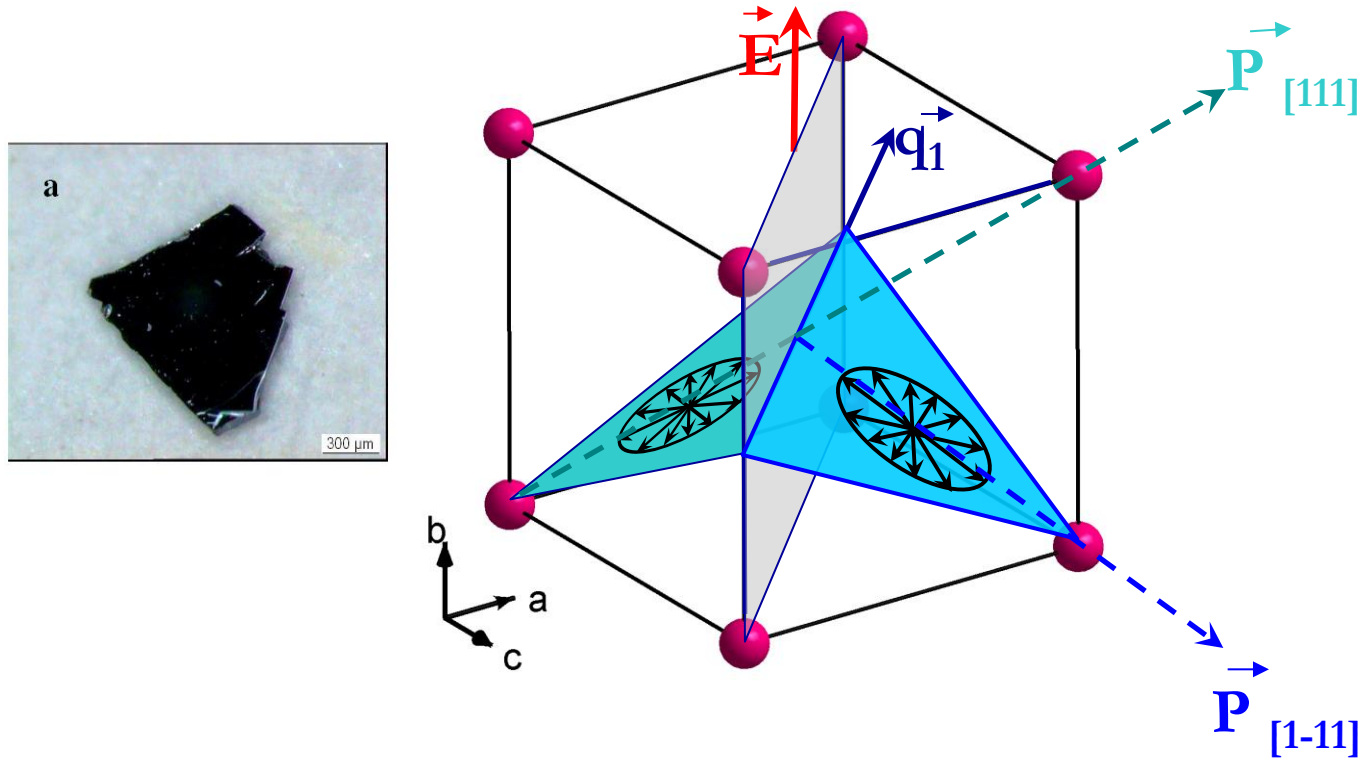
Electric-Field-Induced Spin Flop in BiFeO₃ Single Crystals at Room Temperature

D. Lebeugle,¹ D. Colson,¹ A. Forget,¹ M. Viret,¹ A. M. Bataille,² and A. Gukasov²

¹*Service de Physique de l'Etat Condensé, DSM/IRAMIS, CEA Saclay, F-91191 Gif-Sur-Yvette, France*

²*Laboratoire Leon Brillouin, DSM/IRAMIS, CEA Saclay, F-91191 Gif-Sur-Yvette, France*

(Received 24 January 2008; published 2 June 2008)



Electric-Field-Induced Spin Flop in BiFeO₃ Single Crystals at Room Temperaturenature
materialsFull text access provided to CEA Saclay
by DSI/SITI/CAISTSearch This journal go Advanced search

Journal home > Archive > Research Highlights > Full Text

Journal content

Journal home

Advance online publication

Current issue

Archive

Insight

Focuses

Press releases

Journal information

Guide to authors

Online submission

For referees

Pricing

Contact the journal

Subscribe

Help

About this site

NPG services

Research Highlights

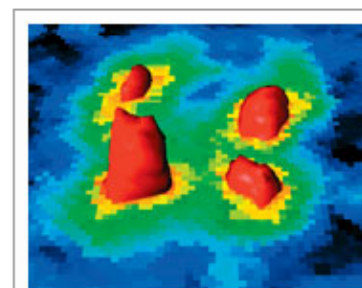
Nature Materials **7**, 517 (2008)
doi:10.1038/nmat2217

Looking, seeing, sensing
A COUPLING, INDEED

top

Phys. Rev. Lett. **100**, 227602 (2008)

One of the most intensively studied multiferroic materials is BiFeO₃, mostly because it shows room-temperature multiferroic coupling with a large spontaneous electric polarization. Although the material has been known to be magnetoelectric since the 1960s, actual evidence of multiferroic coupling in bulk material has been missing, mainly owing to the lack of suitable high-quality crystals. Having achieved the growth of high-quality BiFeO₃ crystals, Delphine Lebeugle and co-workers now report on a neutron diffraction study into the coupling between magnetic and ferroelectric properties of BiFeO₃. They find that although the material has no linear magnetoelectric effect, the antiferromagnetic moments form a low-pitch spiral that creates an efficient multiferroic coupling. However, a more efficient switching of magnetic properties can be achieved not through a direct multiferroic coupling but if the antiferromagnetic moments of BiFeO₃ are used to switch the magnetic moments of a ferromagnet through the exchange interaction at the interface between the two materials. Therefore, an electric field applied to BiFeO₃ indirectly switches the ferromagnetic state of the adjacent layer, as has been demonstrated recently.



MICHEL VIRET

Subscribe to Nature Materials

Subscribe

This issue

- Table of contents
- Previous article
- Next article

Article tools

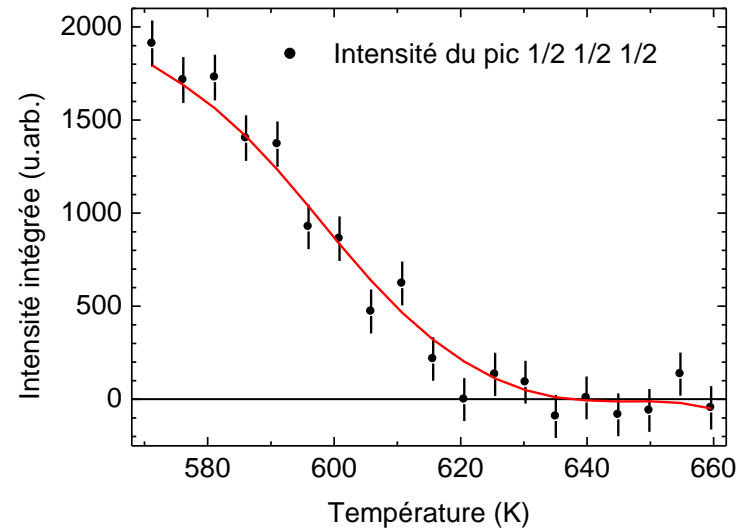
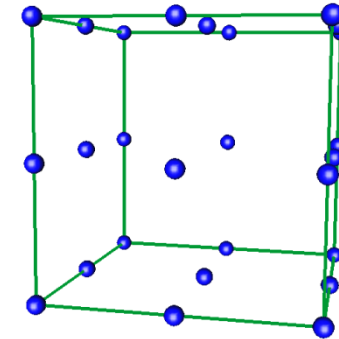
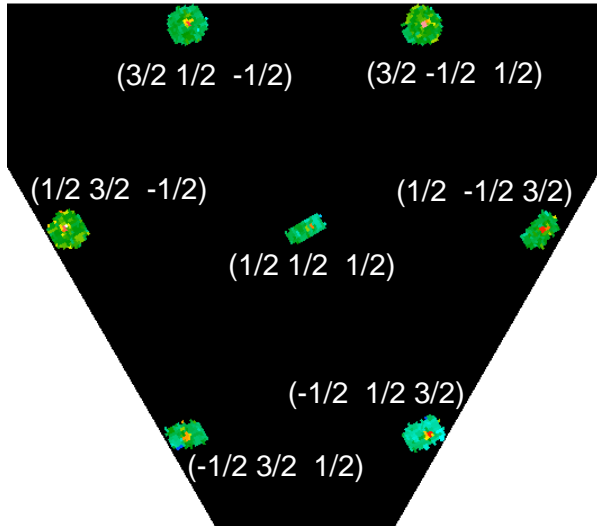
- Download PDF
- Send to a friend
- Export citation
- Rights and permissions
- Order commercial reprints
- Save this link

Article navigation

- Seeing the matrix
- Look very carefully
- A coupling, indeed

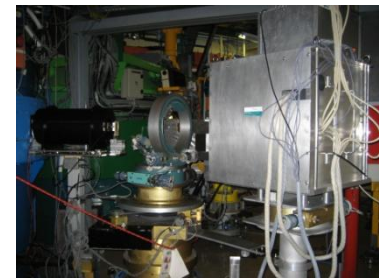
● Epitaxial crystals

BiFeO₃ 90 nm x 1 cm² $V = 0,009 \text{ mm}^3$

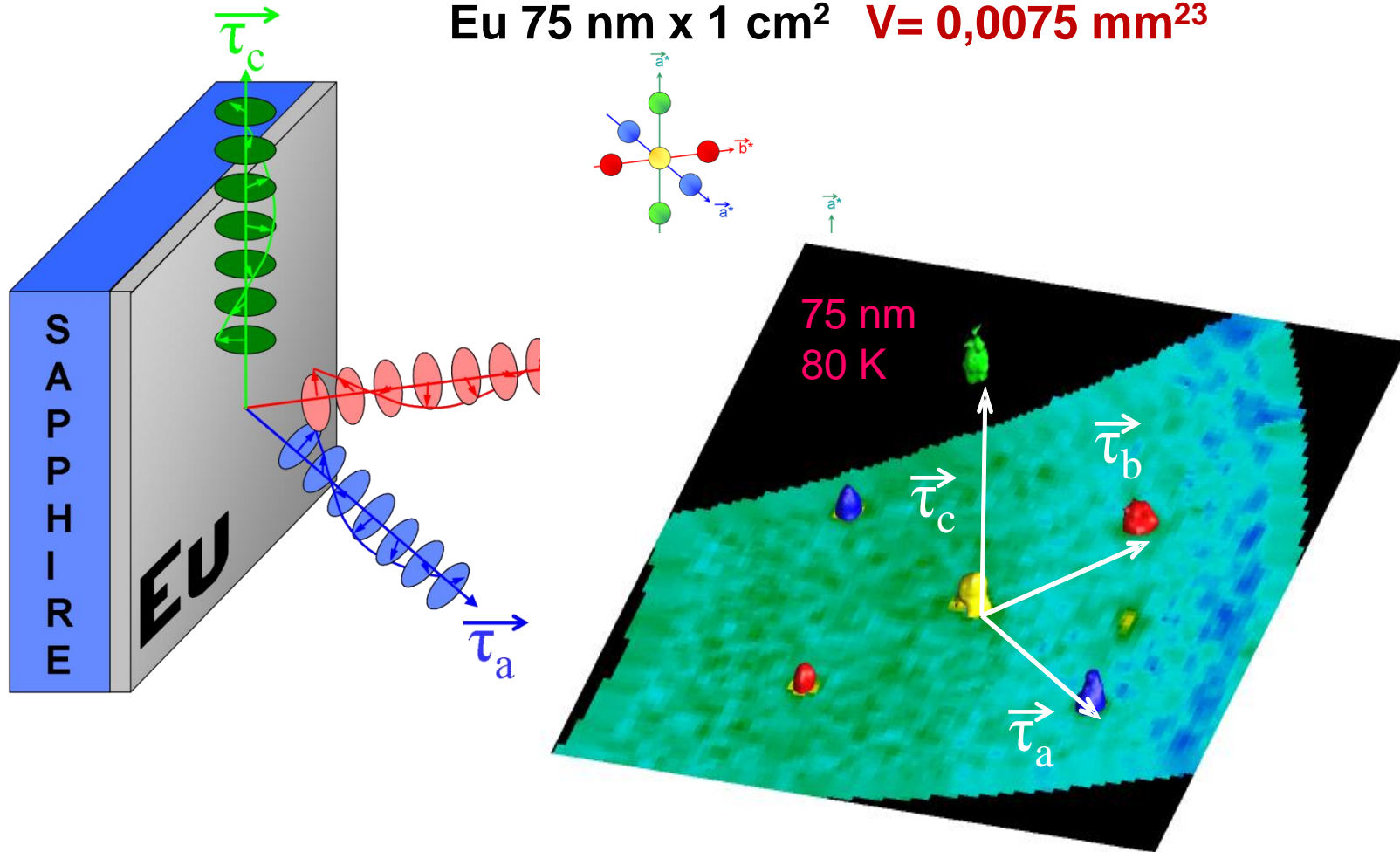


H. Béa *et al.*, *Phil. Mag. Lett.* **87** 165 (2007)
D. Sando *et al.*, *Nature Mat.* **12** 641 (2013)

● Epitaxial crystals

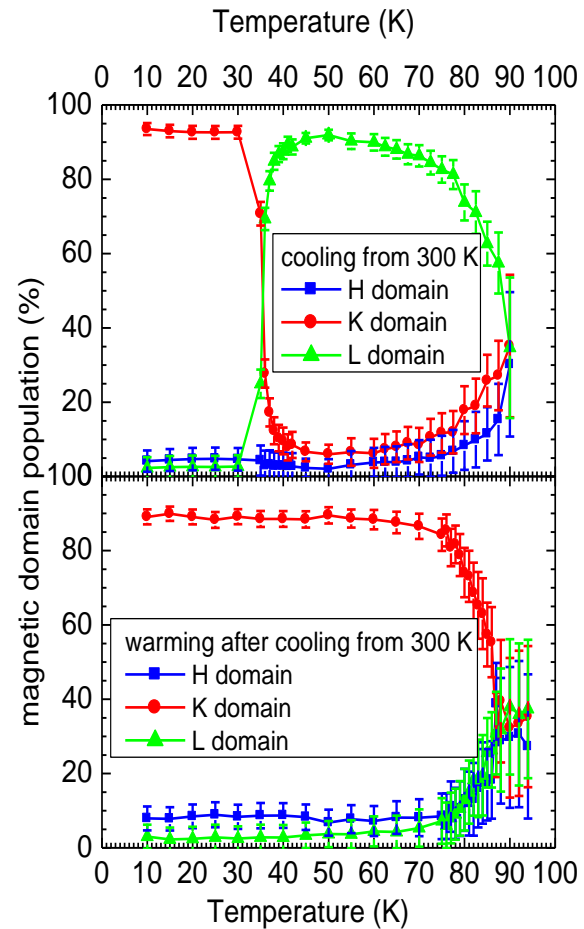
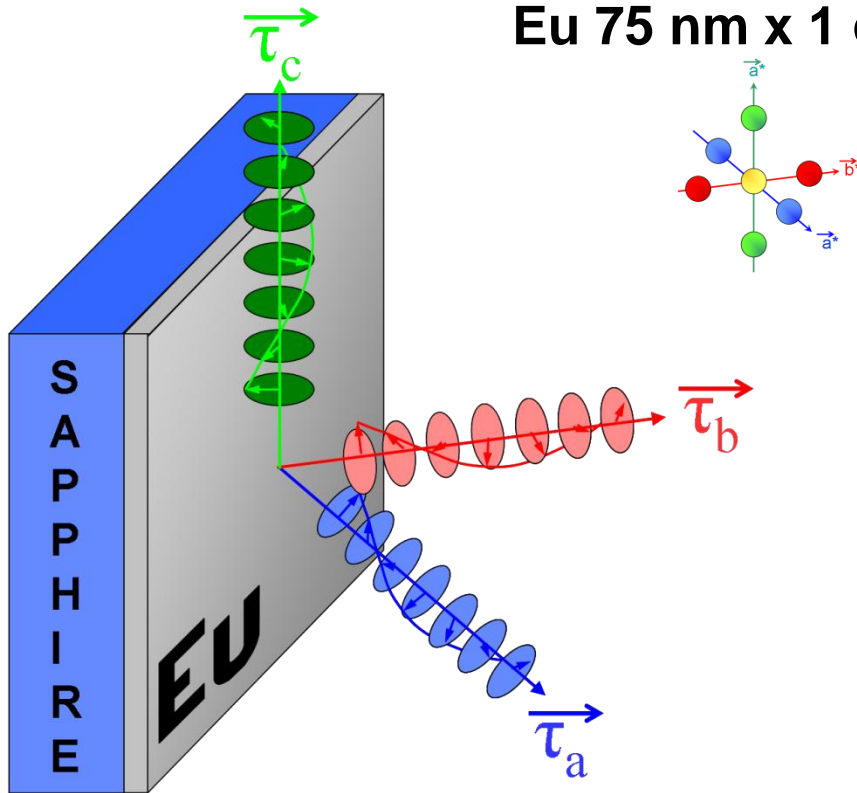


Eu 75 nm x 1 cm² $V = 0,0075 \text{ mm}^3$



● Epitaxial crystals

Eu 75 nm x 1 cm² $V = 0,0075 \text{ mm}^3$



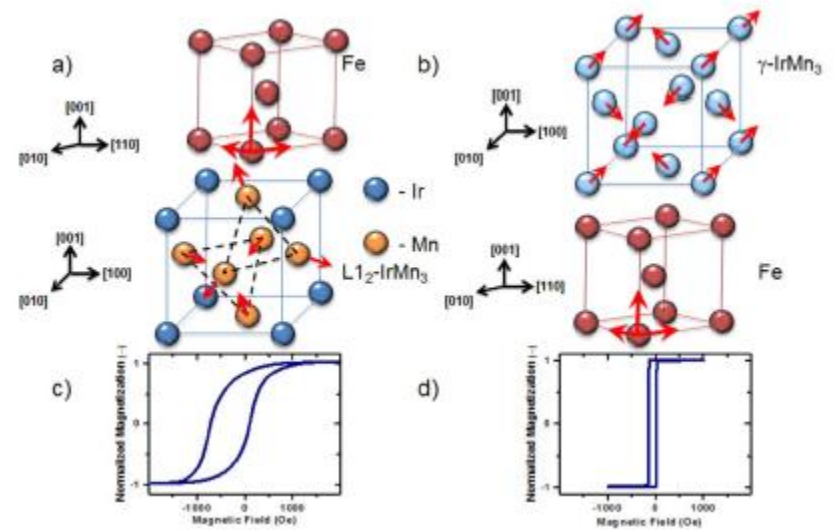
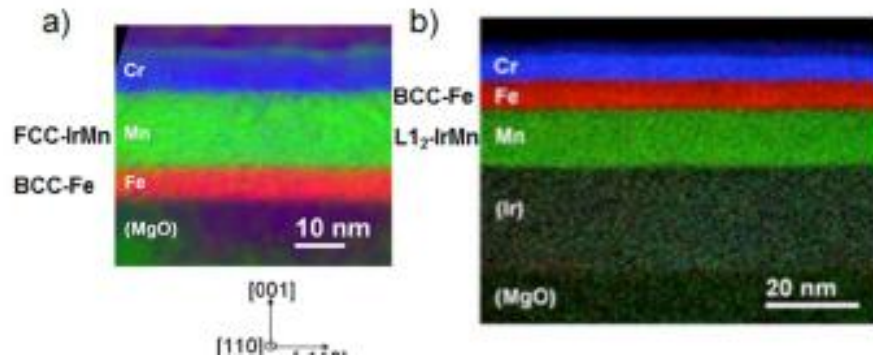
● Epitaxial crystals

OPEN

The antiferromagnetic structures of IrMn_3 and their influence on exchange-bias

SUBJECT AREAS:
TRANSMISSION
ELECTRON MICROSCOPY

A. Kohn^{1,2}, A. Kovács³, R. Fan⁴, G. J. McIntyre⁵, R. C. C. Ward⁶ & J. P. Goff⁷

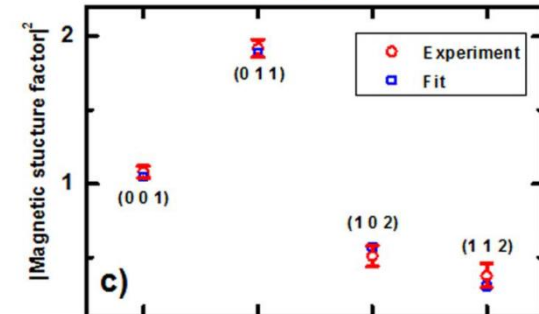
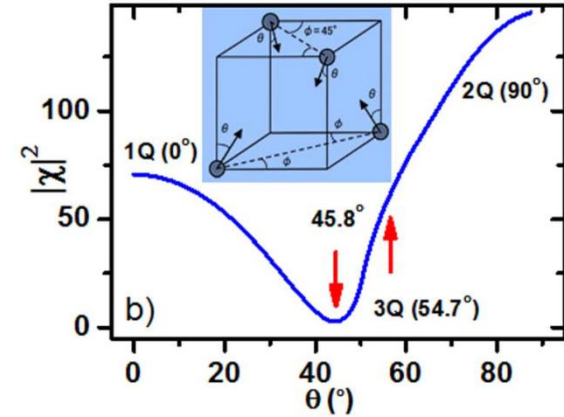
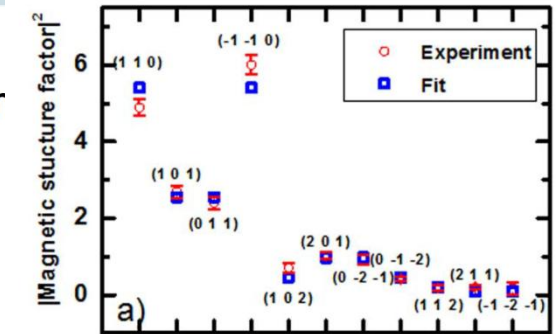
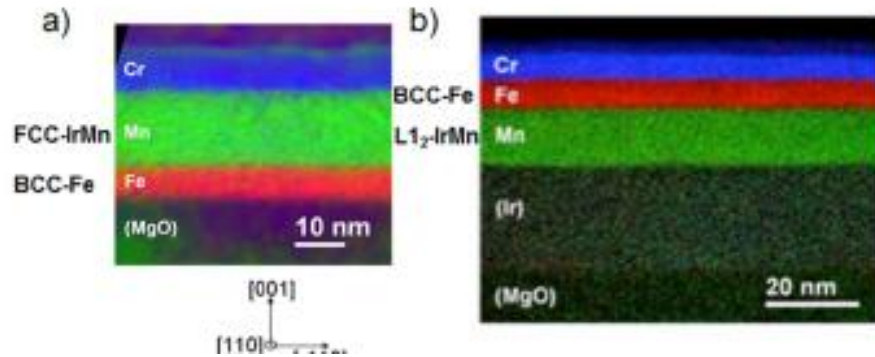


OPEN

The antiferromagnetic structures of IrMn and their influence on exchange-bias

SUBJECT AREAS:
TRANSMISSION
ELECTRON MICROSCOPY

A. Kohn^{1,2}, A. Kovács³, R. Fan⁴, G. J. McIntyre⁵, R. C. C. Ward⁶ & J. P. Goff⁷



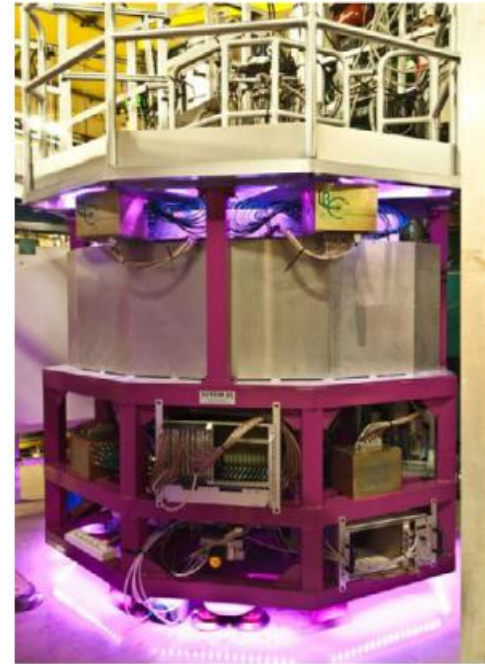
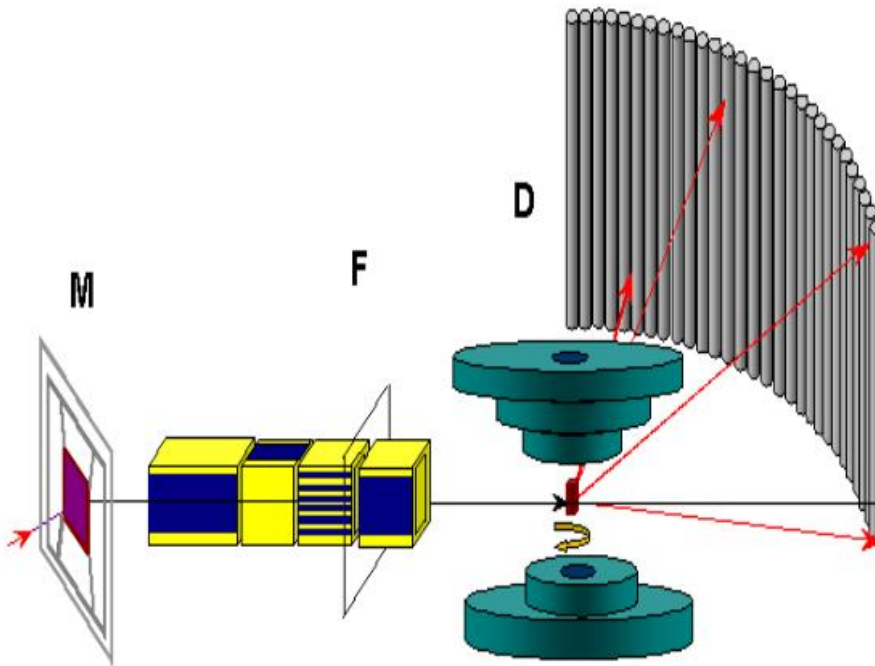
● Epitaxial crystals

Eu 75 nm x 1 cm² V= 0,0075 mm³

Practical volume now > 0.01 mm³ only CN

2-3 orders of magnitude smaller needed HN

VIP Neutron DIFFRACTOMETER (5C1) LLB



$80^\circ \times 25^\circ$, $\lambda = 0.84 \text{ \AA}$

VIP Neutron DIFFRACTOMETER (5C1) LLB

Yb₂Ti₂O₇ 2 K, 1 T
V~60mm³

3500 steps of 0.1
Exposition 4 sec/frame

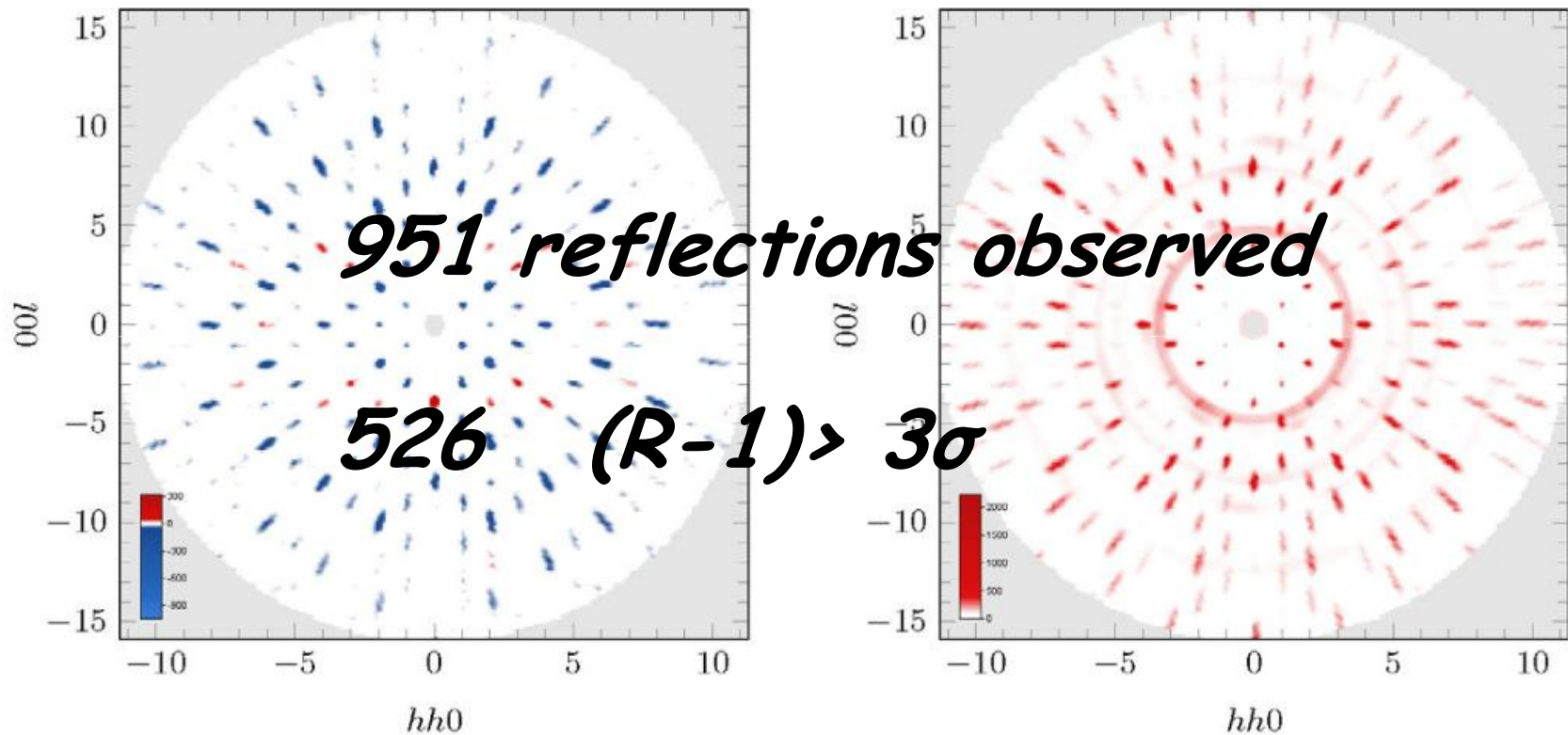
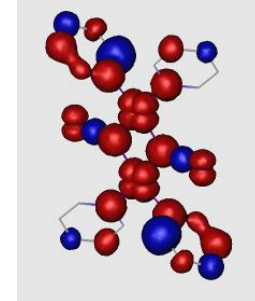
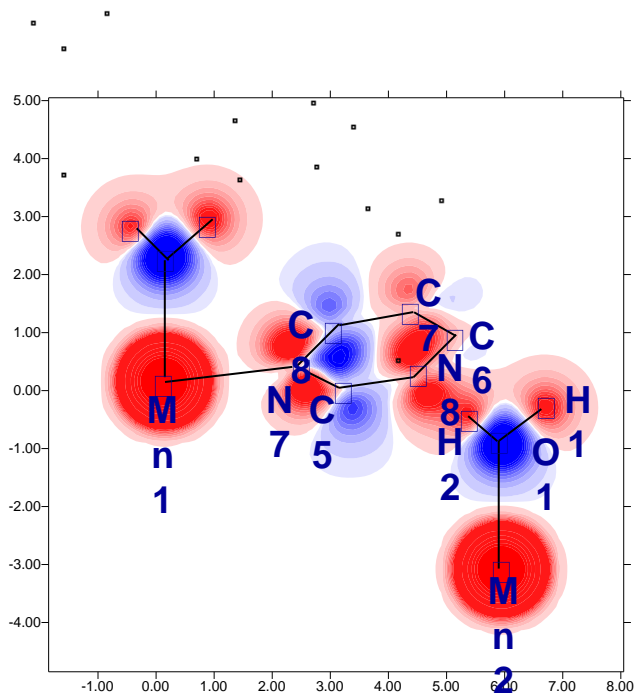


Fig. 3. Two dimensional cuts in the reciprocal space measured on VIP from Yb₂Ti₂O₇ (about 100 mm³) during 5 hours. Left panel: The difference $F' - F$. Right panel: The sum $F' + F$.

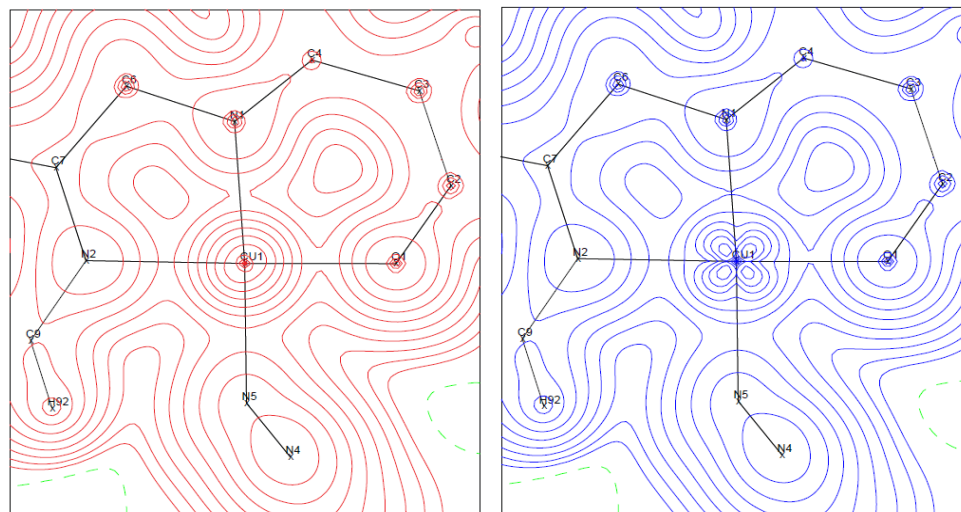
● Molecular Magnetism



SPIN DENSITY



JOINT X-PND REFINEMENT



Spin up

Spin down

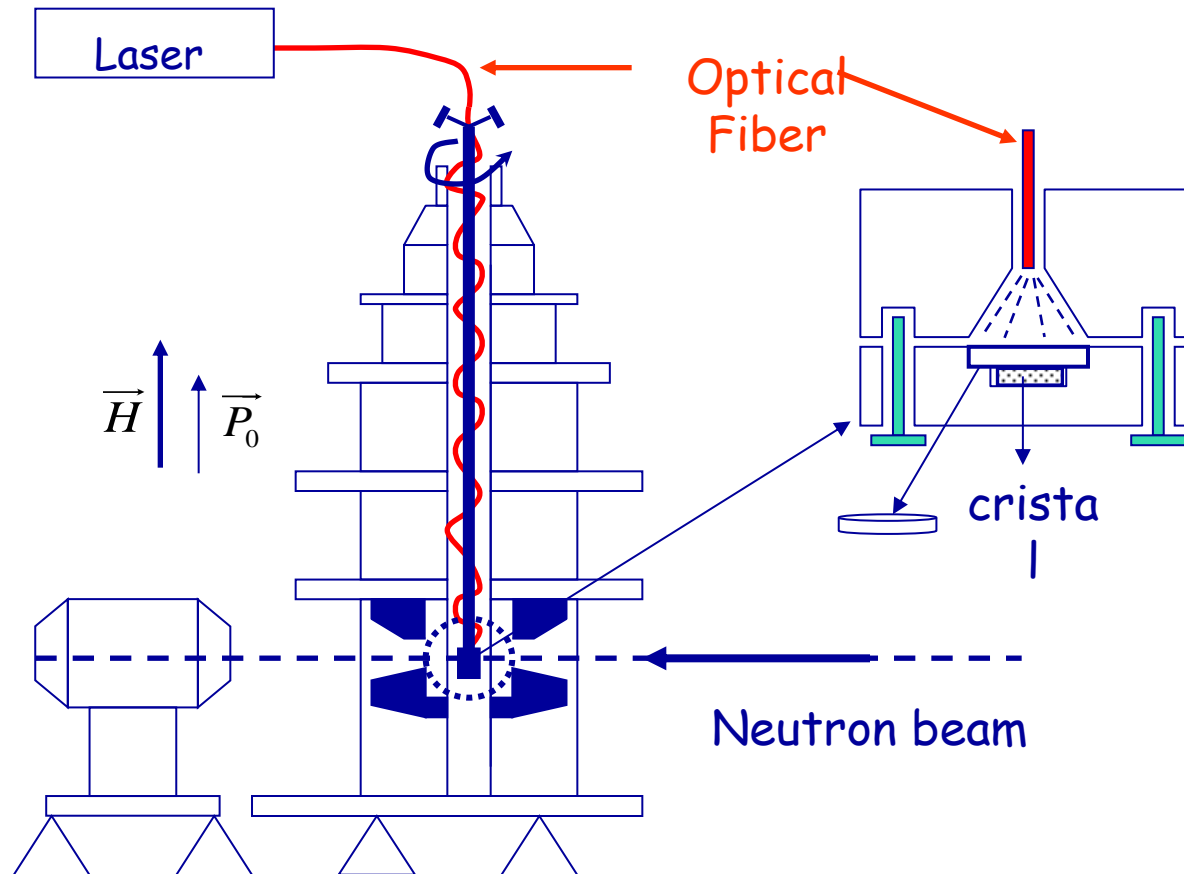
N₂(CH)₄ (pyrimidine)_h

B. Gillon et al.

M. Deutch et al.

● Molecular Magnetism

Photocrystallography

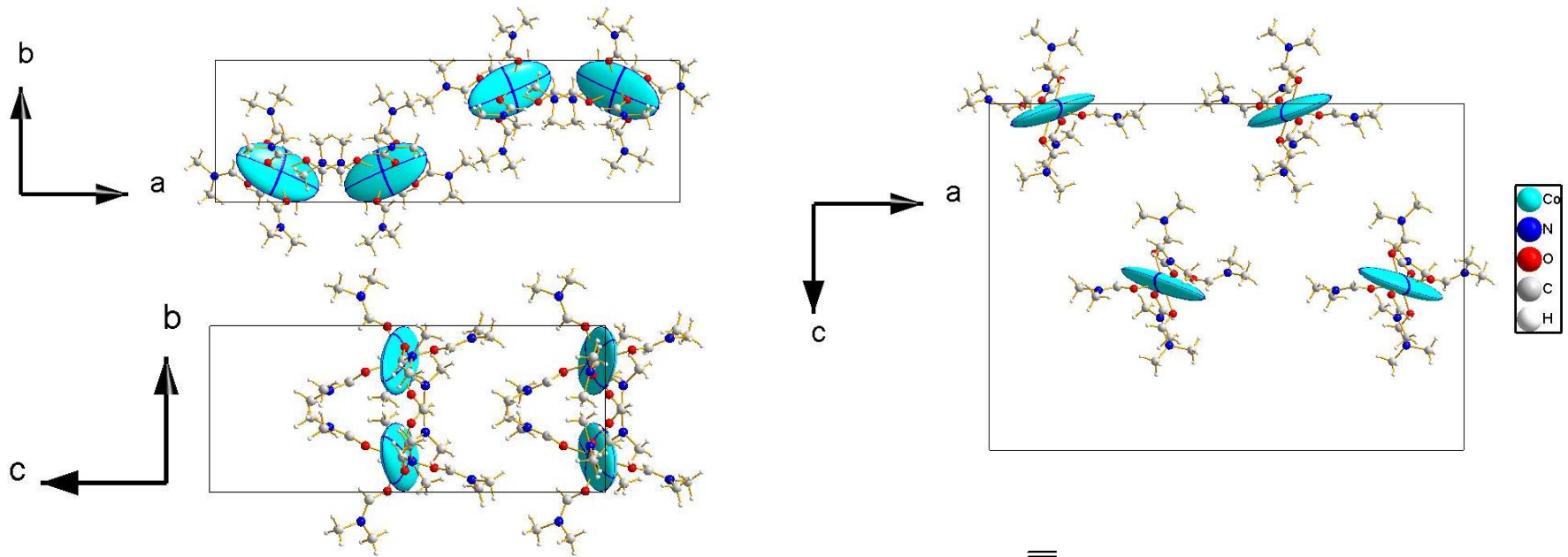


● Molecular Magnetism

Practical volume now $> 10 \text{ mm}^3$ **HN** (**CN**)

3 orders of magnitude smaller needed HN

Local Anisotropy in the complex [Co²⁺(DMF)₆]



$$\vec{m} = \overline{\chi} \vec{H}$$

$$\vec{F}_M(\vec{Q}) = \sum_k^{atoms} \overline{\chi}_k \vec{H} f_k(\vec{Q}) \exp(i\vec{Q} \cdot \vec{r}_k)$$

Determination of atomic site susceptibility tensors from polarized neutron diffraction data

A Gukasov¹ and P J Brown²

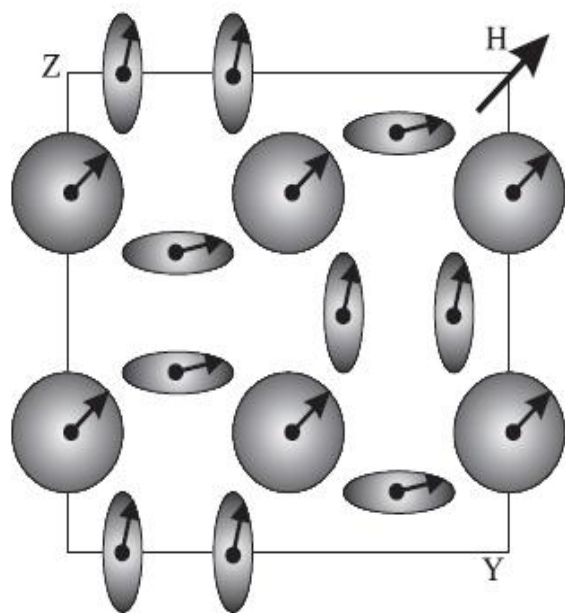
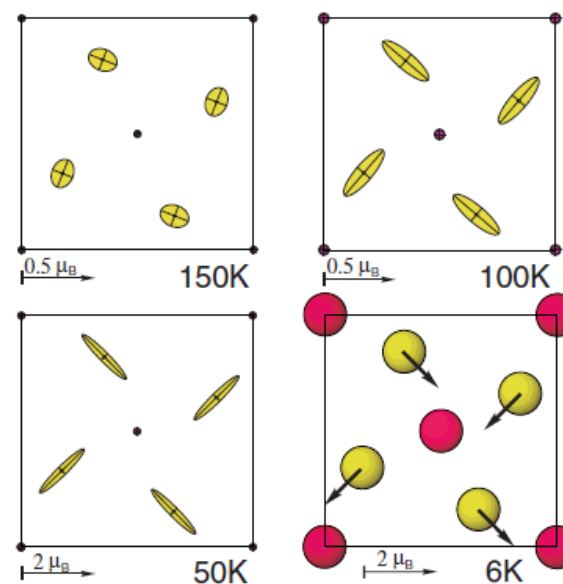


Figure 4. The [100] projection of the unit cell of $\text{Nd}_{3-x}\text{S}_4$ for $H \parallel [011]$.

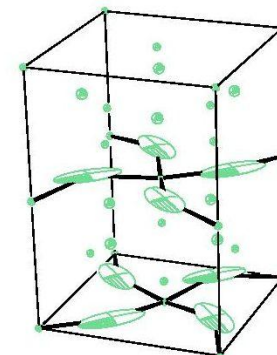
Site susceptibility tensors and magnetic structure of $\text{U}_3\text{Al}_2\text{Si}_3$: a polarized neutron diffraction study

A G Gukasov¹, P Rogl², P J Brown³, M Mihalik⁴ and A Menovsky⁵



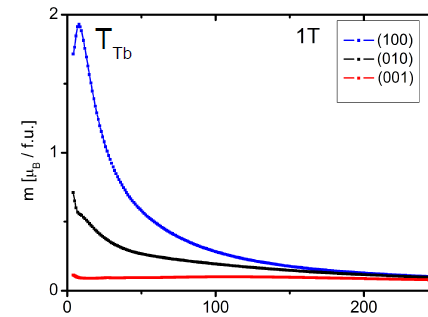
● U1 (0 0 1/4) ● U2 (0 0 3/4) ● U3 (0.15f)

Figure 3. Evolution with temperature of the magnetic anisotropy



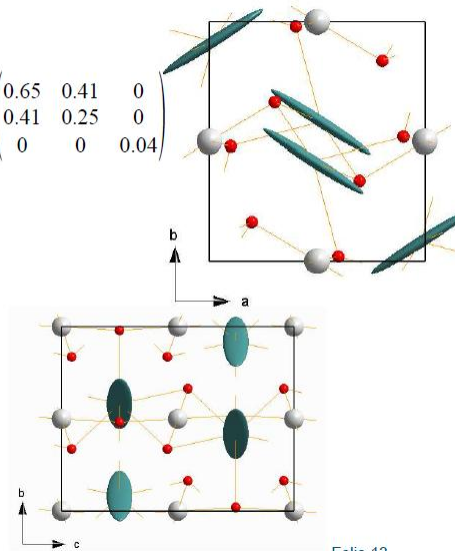
● Multiferroics

● TbMnO₃



T=50K

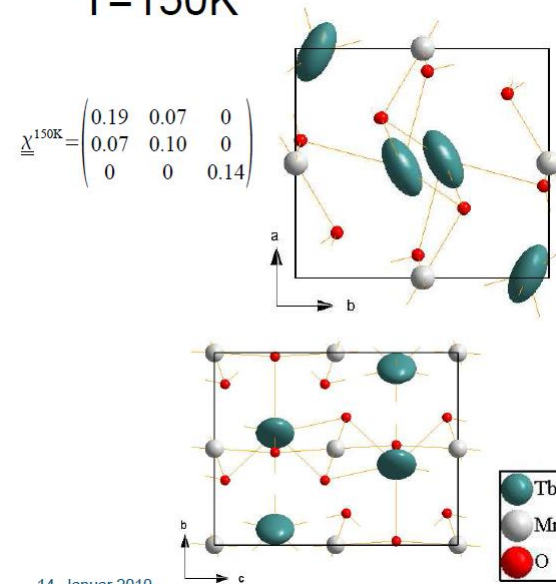
$$\underline{\chi}^{50K} = \begin{pmatrix} 0.65 & 0.41 & 0 \\ 0.41 & 0.25 & 0 \\ 0 & 0 & 0.04 \end{pmatrix}$$



Folie 13

T=150K

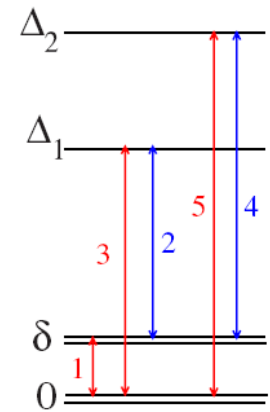
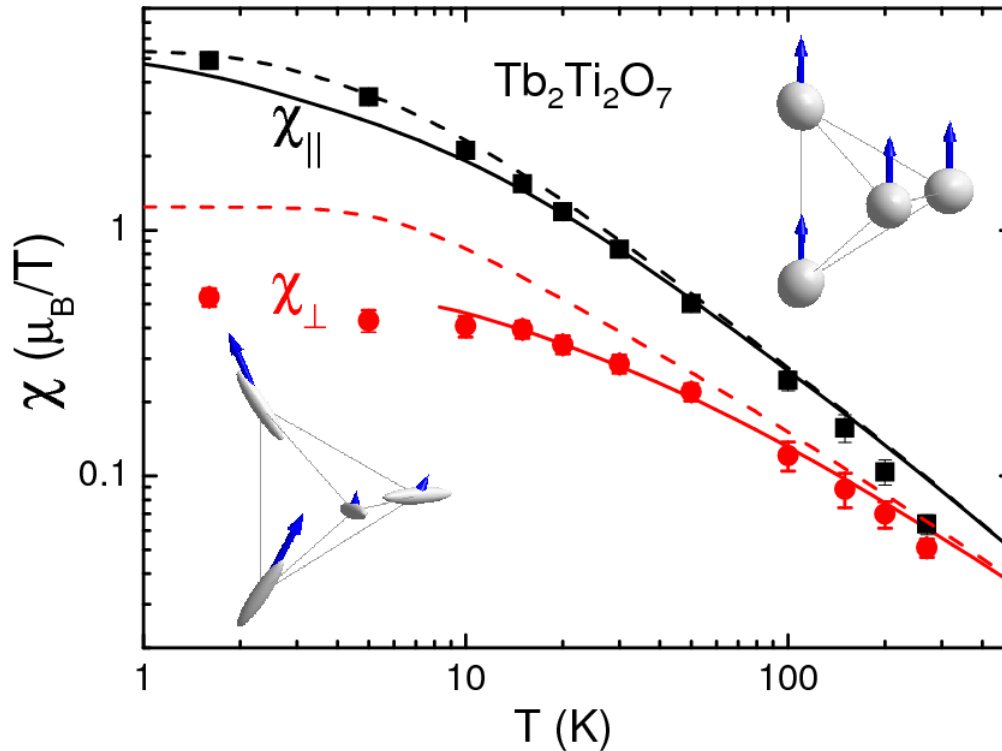
$$\underline{\chi}^{150K} = \begin{pmatrix} 0.19 & 0.07 & 0 \\ 0.07 & 0.10 & 0 \\ 0 & 0 & 0.14 \end{pmatrix}$$



14. Januar 2010

Soft-Ising (Spin Liquid Tb2Ti2O7)

Lines shows fit using CF parameters from inelastic neutrons for Tb2Ti2O7.
 I. Mirebeau, M. Hennion and P. Bonville . Phys Rev. B 184436, 2007

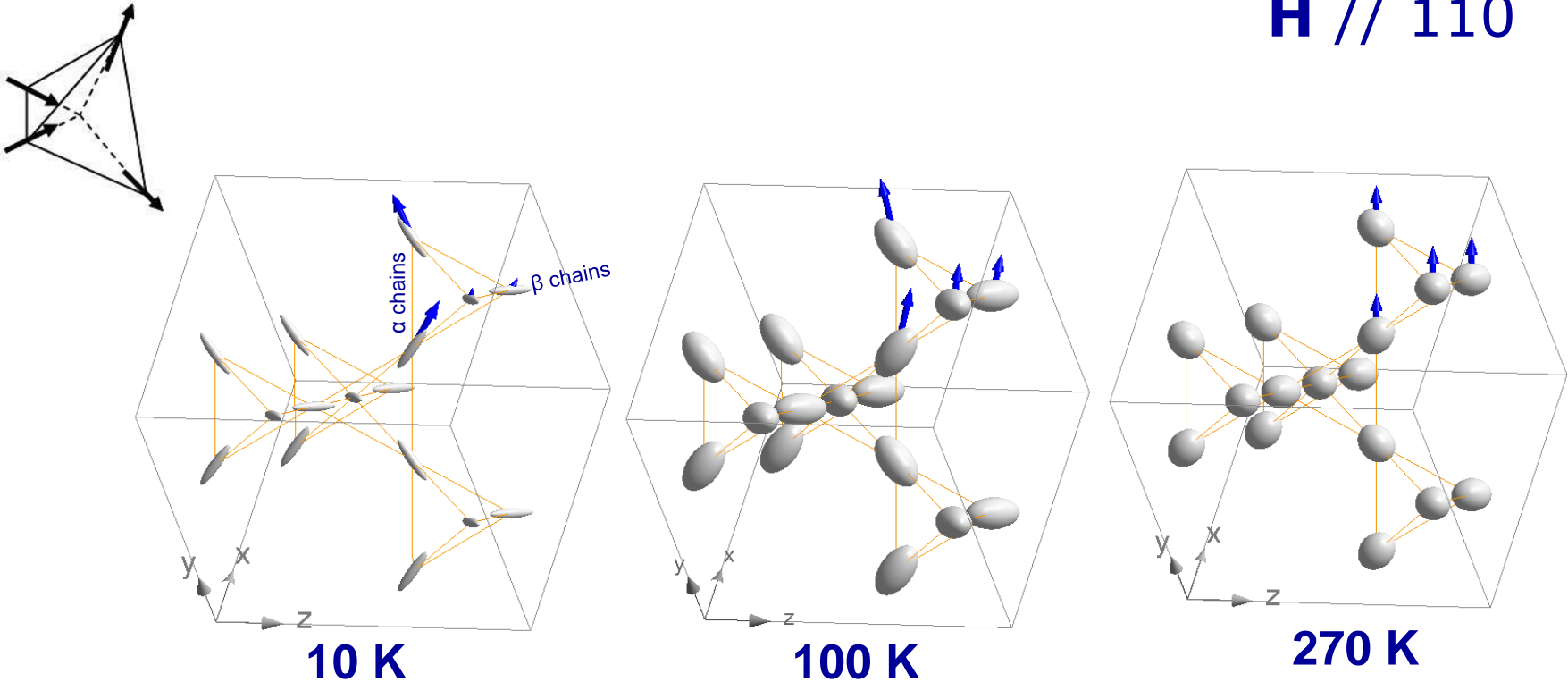


$\delta \approx 15$ K

$$M_i = \chi_{ij} H_j + \lambda \langle M_j \rangle$$

FROM HEISENBERG TO ISING BEHAVIOR

$\mathbf{H} // 110$



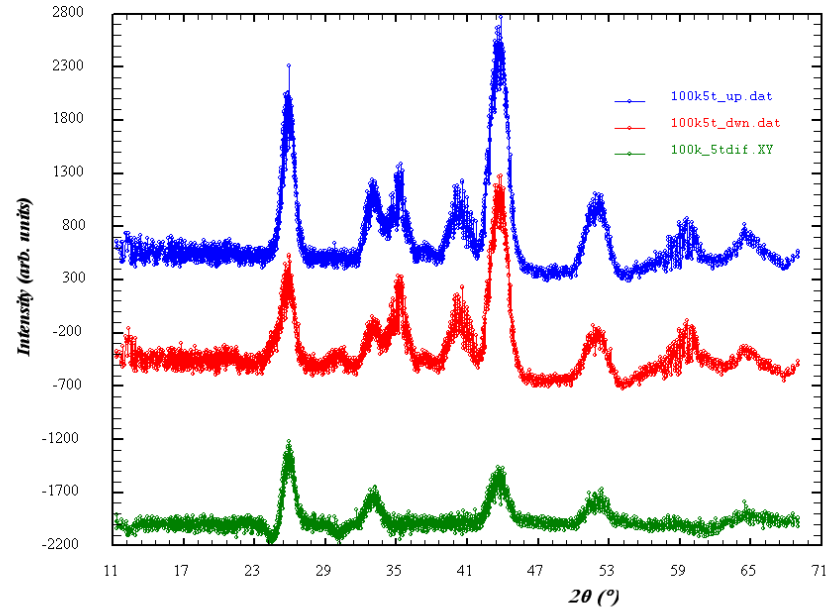
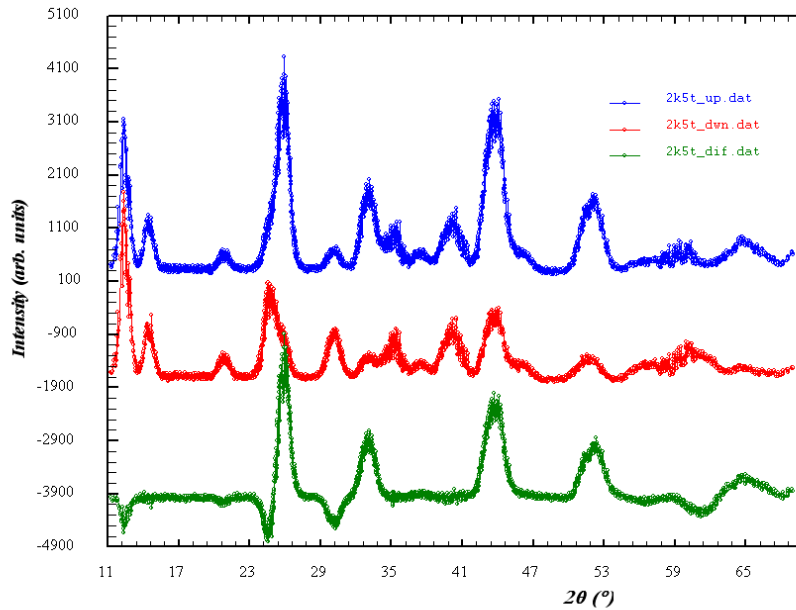
Ellipsoids are multiplied by T to compensate Curie-Weiss behavior

ASPs on Powder

Tb₂Sn₂O₇

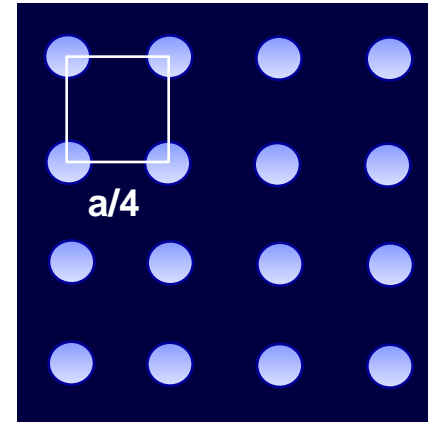
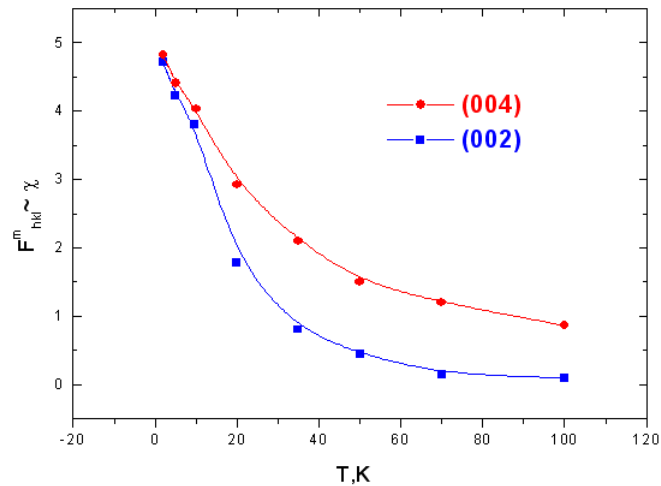
2k 5T

100k 5T



ASPs using Unpolarized Neutrons

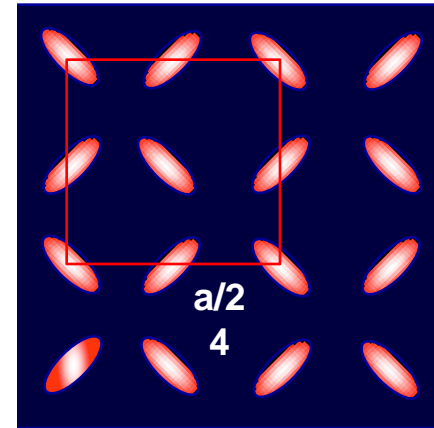
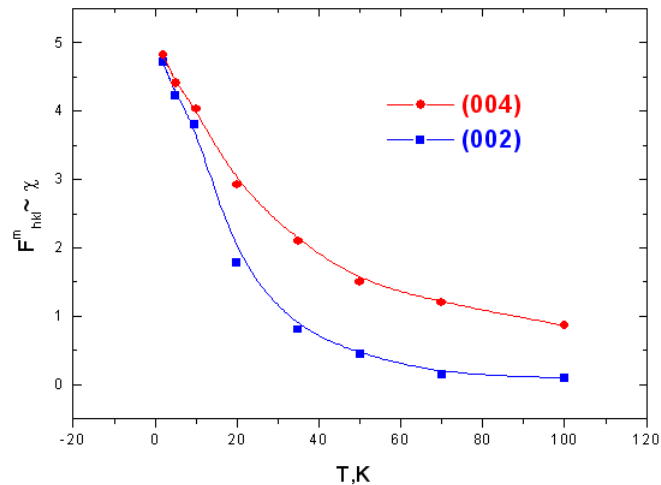
Extinction rules for pyrochlore impose **Fd-3m**
(00h)=4n



$I_m(400) \sim \chi_{11}$ Heisenberg behavior

ASPs using Unpolarized Neutrons

Lattice is doubled under magnetic field
(200) appears



$I_m(400) \sim \chi_{11}$ Heisenberg behavior

$I_m(200) \sim \chi_{12}$ Ising or XY behavior

FAST TRACK COMMUNICATION

Determination of atomic site susceptibility tensors from neutron diffraction data on polycrystalline samples

A Gukasov¹ and P J Brown²

$$\begin{aligned}
 \langle |M_{\perp}(\mathbf{k})|^2 \rangle &= \frac{H^2}{\pi} \int_{-\pi/2}^{\pi/2} |M_{\perp}(\mathbf{k})|^2 d\psi \\
 &= \frac{H^2}{\pi} \left[\left(\frac{\Xi_{11}^2 + \Xi_{22}^2}{2} + \Xi_{12}^2 \right) \psi + \left(\frac{\Xi_{12}(\Xi_{11} + \Xi_{22})}{2} \right) \cos 2\psi \right]_{-\pi/2}^{\pi/2} \\
 &= H^2 \left(\frac{\Xi_{11}^2 + \Xi_{22}^2}{2} + \Xi_{12}^2 \right) \quad (7)
 \end{aligned}$$

and the mean value of $M_{\perp}(\mathbf{k}) \cdot \mathbf{P}$ is

$$\begin{aligned}
 \langle M_{\perp}(\mathbf{k}) \cdot \mathbf{P} \rangle &= \frac{PH}{\pi} \int_{-\pi/2}^{\pi/2} \left(\Xi_{11} \cos^2 \psi + 2\Xi_{12} \sin \psi \cos \psi + \Xi_{22} \sin^2 \psi \right) d\psi \\
 &= \frac{PH}{\pi} \left[\left(\frac{\Xi_{11} + \Xi_{22}}{2} \right) \psi + \Xi_{12} \cos 2\psi \right]_{-\pi/2}^{\pi/2}
 \end{aligned}$$

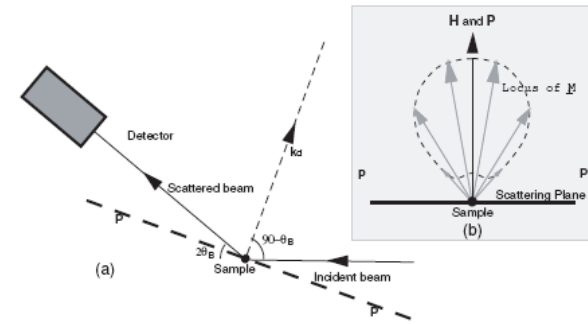
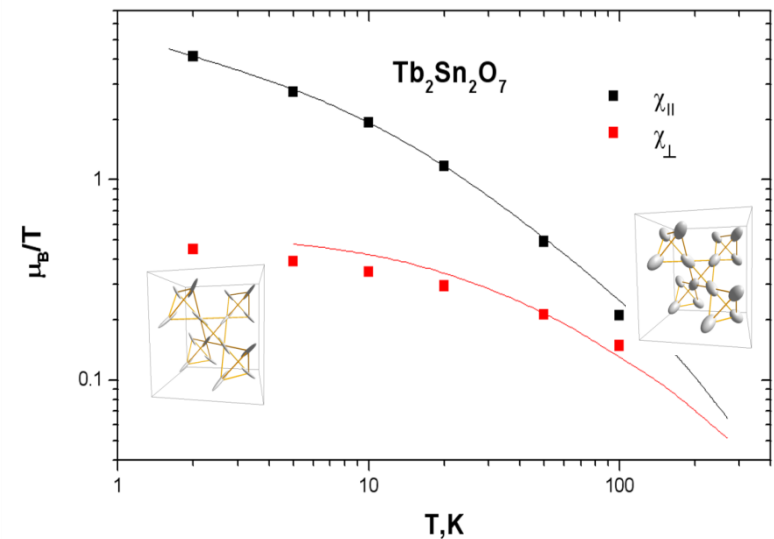


Figure 1: (a) Section in the scattering plane perpendicular to the polarisation and magnetic field direction showing the geometry for scattering by a polycrystalline sample. (b) The shaded inset shows the plane perpendicular to the scattering vector \mathbf{k}_s of a reflection and indicates the locus of the magnetic interaction vectors of different contributing grains



CHILSQ program in CCSL (P J Brown)

WAITING FOR FULLPROF

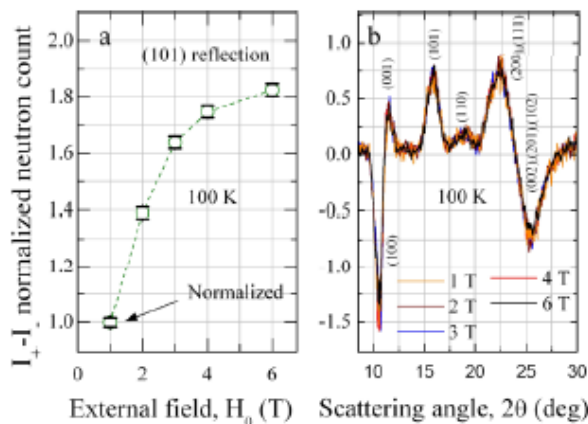
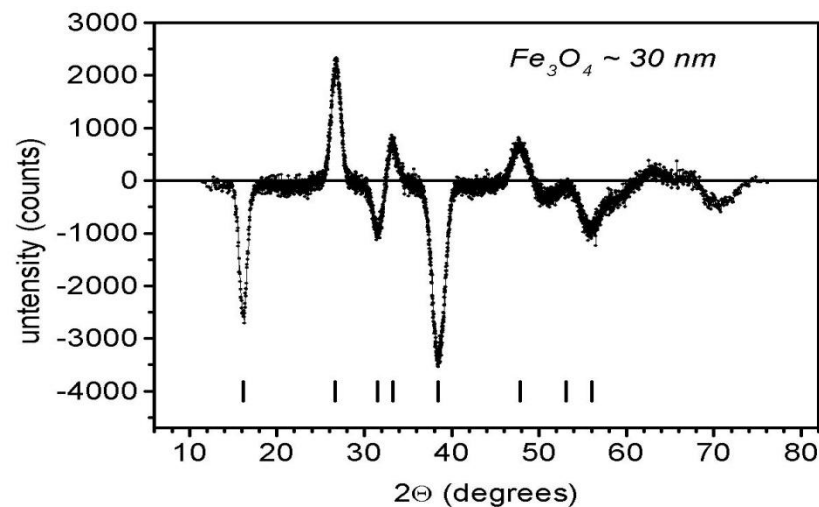


Fig. 6. This figure is reconstructed from data collected in a study of TbCo_2Ni_3 [13]. The 100 K observed (a) (101) reflection's integrated count H_0 dependence, normalized to that observed at $H_0 = 1$ T (the dashed line is a guide to the eye) and (b) the flipping difference, $I_+ - I_-$, profile, normalized to the (101) reflection's integrated count, under the influence of different magnitude external magnetic fields, (1 T – orange, 2 T – brown, 3 T – blue, 4 T – red and 6 T – black). (The colors are visible in the online version of the article; <http://dx.doi.org/10.3233/JNR-140015>.)



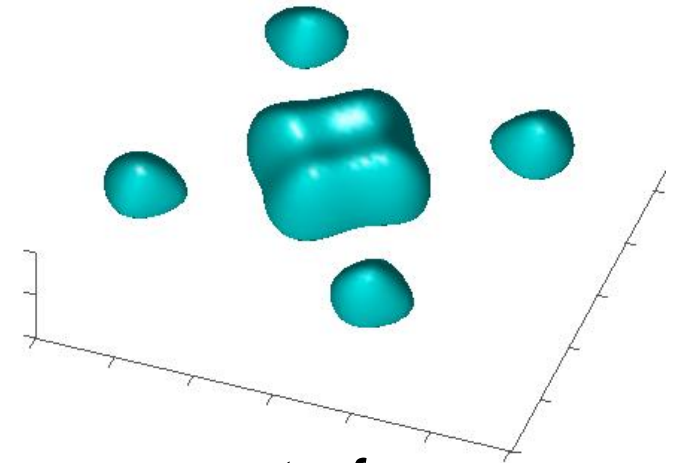
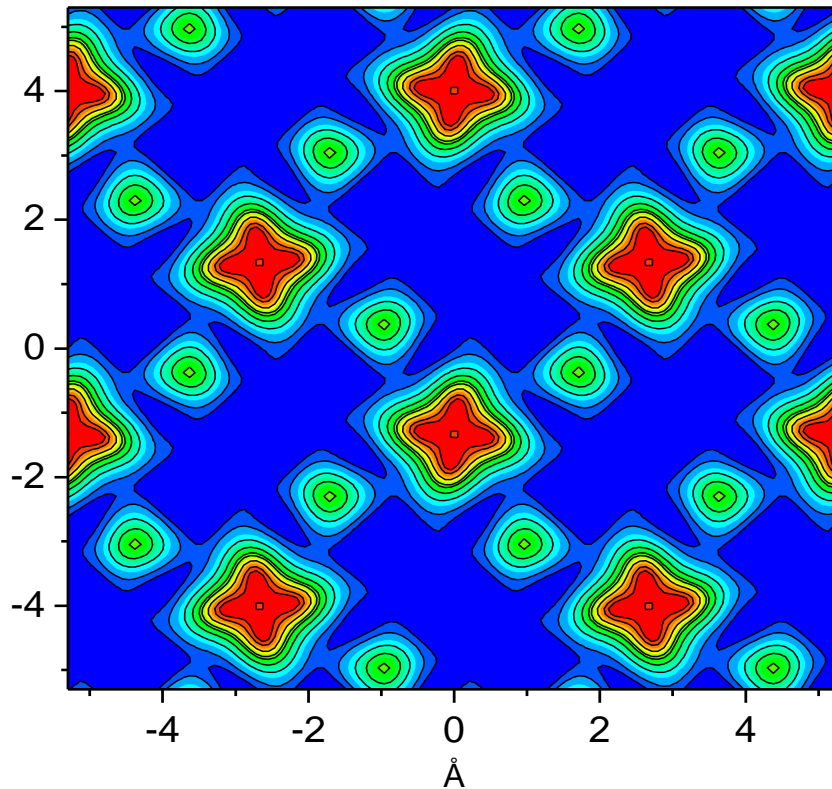
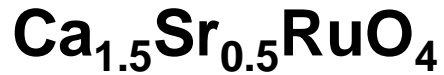
Local Anisotropy

Practical volume now $> 10 \text{ mm}^3$ **HN (CN)**

3 days for full temperature dependence

Should be not more than several hours to work as a local (site) Magnetometer

● Superconductivity



Large amount of magnetization on Oxygen

- 0.35 μ_B** Ruthenium
- 0.08 μ_B** Oxygen (in-plane)
- 0.01 μ_B** Oxygen (apical)

A. Gukasov, M Braden, R J Papoular, S Nakatsuji and Y Maeno .
PRL89, 87202

● Superconductivity

PHYSICAL REVIEW B 88, 184413 (2013)

Magnetization distribution and orbital moment in the nonsuperconducting chalcogenide compound $\text{K}_{0.8}\text{Fe}_{1.6}\text{Se}_2$

S. Nandi,^{1,2,*} Y. Xiao,¹ Y. Su,² L. C. Chabon,³ T. Chatterji,³ W. T. Jin,^{1,2} S. Price,¹ T. Wolf,⁴ P. J. Brown,^{5,3} and Th. Brückel^{1,2}

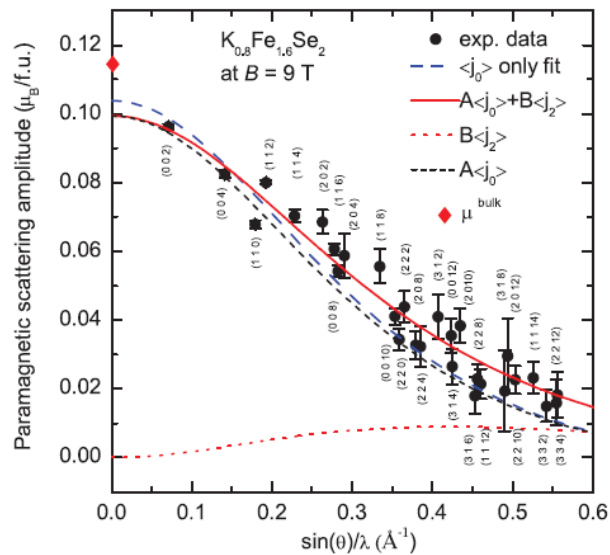


FIG. 2. (Color online) Paramagnetic scattering amplitudes of Fe at $T = 600$ K. The large-dashed curve (blue) shows fitting using the $\langle j_0 \rangle$ form factor for Fe^{2+} , Ref. 27. The solid (red) curve shows fitting with $\langle j_0 \rangle$ and $\langle j_2 \rangle$ form factors with individual contributions are indicated by short-dashed (black) and dotted (red) lines, respectively.²⁸ A and B are fitting parameters.

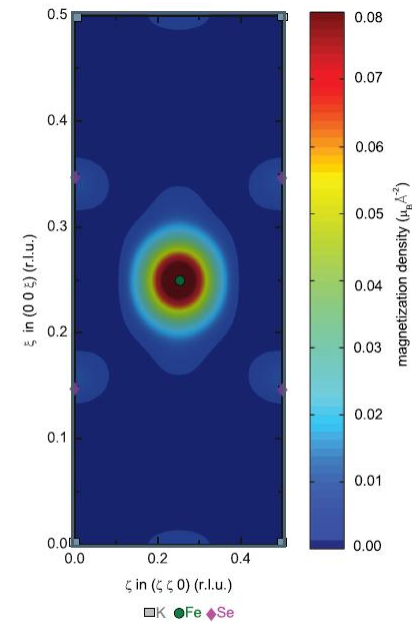


FIG. 3. (Color online) Maximum-entropy reconstruction of the magnetization distribution in tetragonal $\text{K}_{0.8}\text{Fe}_{1.6}\text{Se}_2$ at 600 K projected down to $[1\ 1\ 0]$.

$3d\ t_{2g}$ type; 66% in xz/yz symmetry

● Superconductivity

Varma loops

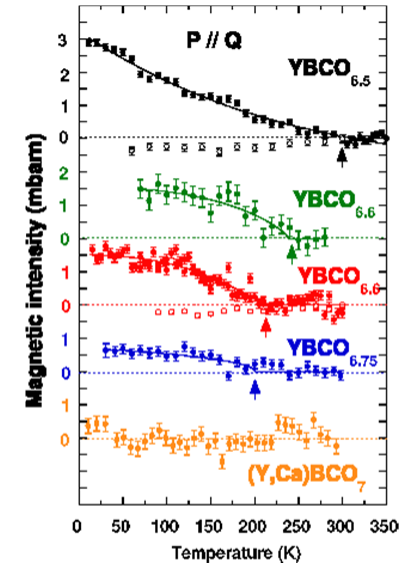
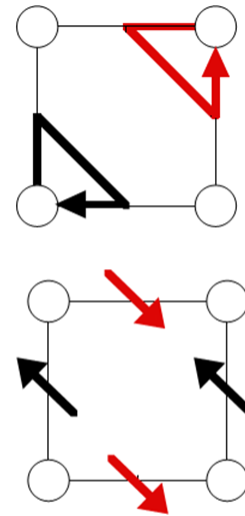
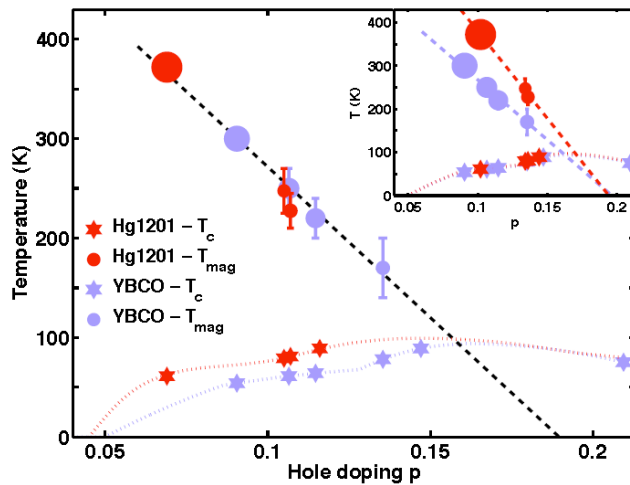


Figure 1 (from [Fau06]): right side) Magnetic intensity measured from the polarized neutron experiment on 4F1 (LLB) on 5 different YBCO samples corresponding to 5 increasing doping from underdoped (YBCO_{6.5}) to overdoped (Y,Ca)BCO₇. The behavior matches the evolution of the pseudogap determined by resistivity data. left side) CuO₂ plaquette where only the Cu atoms are represented showing two intra-unit cell magnetic orders. The upper panel shows the loop current model proposed by Varma [Var06]. The lower panel shows a magnetic model with moments (spin or orbital) at the oxygen sites. Both models can account for the experimental data.

V. Balédent, et al. *Phys. Rev. Lett.* **105**, 027004 (2010).

- **Superconductivity**

Practical volume now > 100 mm³ CN

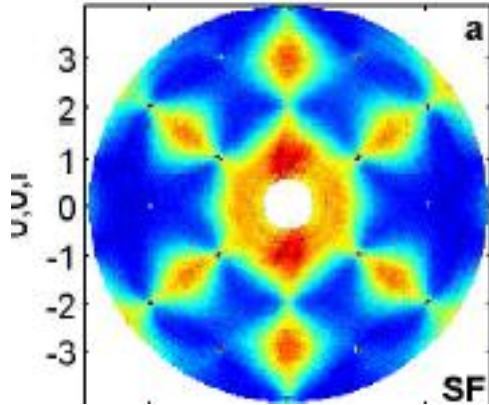
For non superconducting samples

2-3 orders needed

HN

● Frustrated Magnets

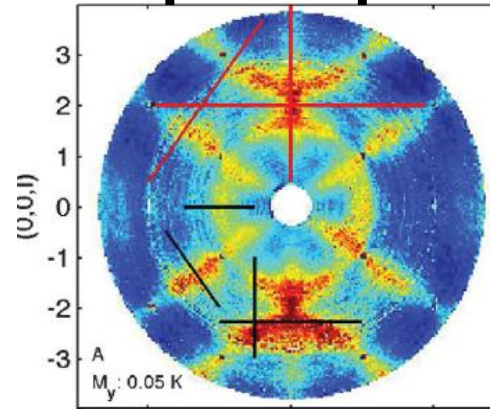
Spin Ice



D7 NPA

6T2 PSD

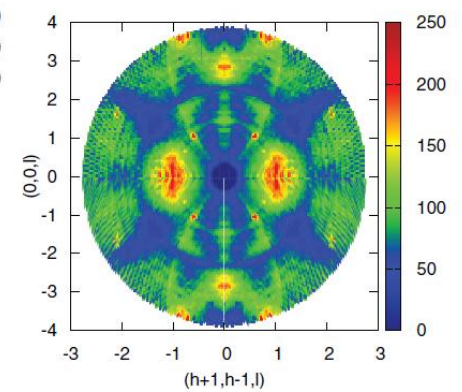
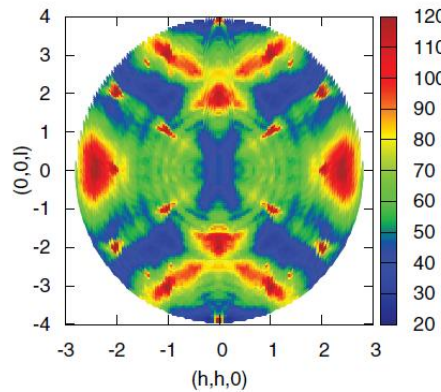
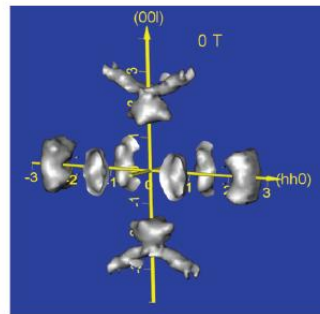
Spin Liquid



Spin Liquid

P. BONVILLE, A. GUKASOV, I. MIREBEAU, AND S. PETIT

PHYSICAL REVIEW B 89, 085115 (2014)



TOWARDS A MODEL OF A DYNAMICAL JAHN-TELLER ...

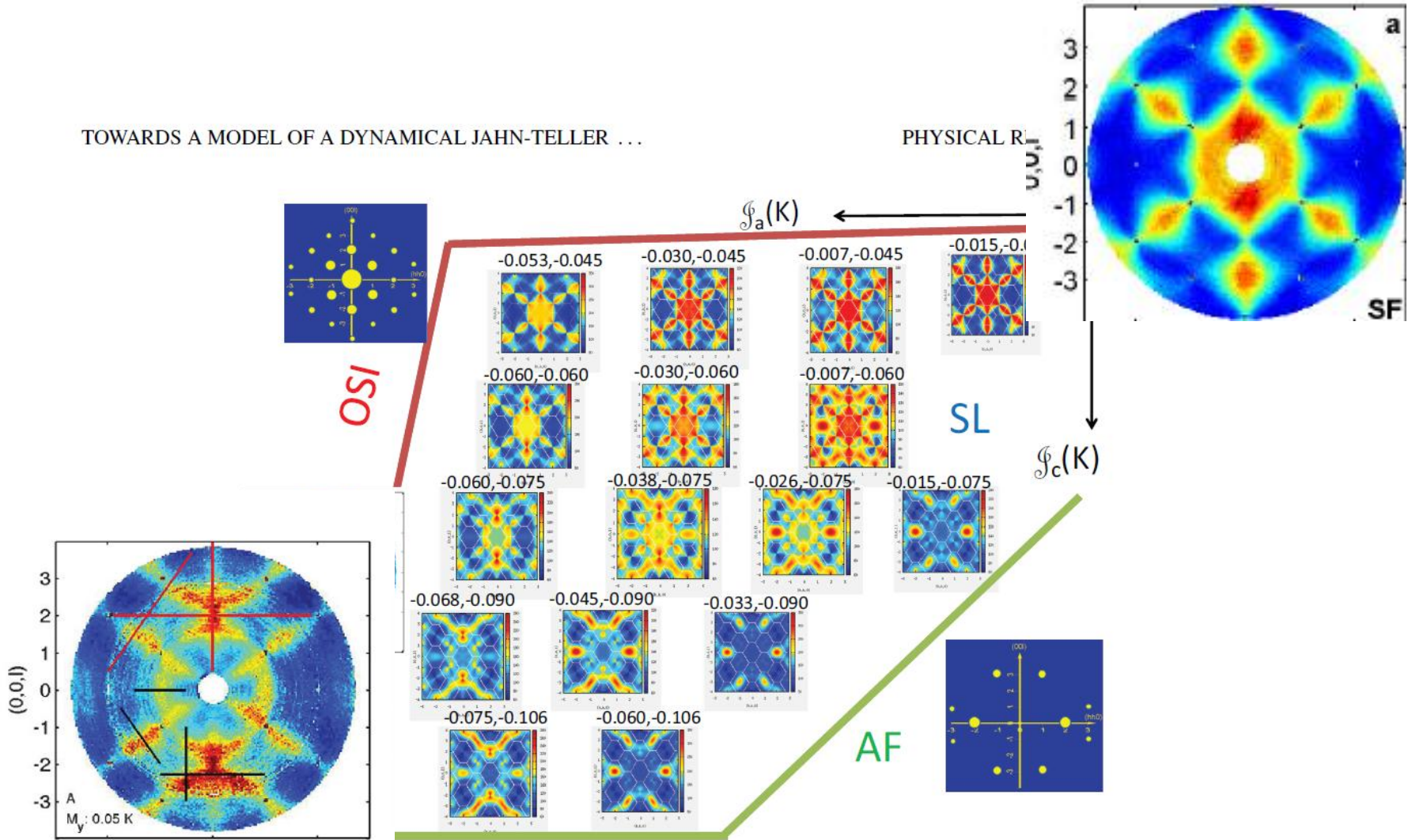


FIG. 4. (Color online) Calculated diffuse scattering maps in the (hhl) plane of the reciprocal space for the spin-flip channel at 0.05 K, according to the geometrical setup of Ref. [20]. The \mathbf{q} maps are represented in the spin liquid (SL) phase of our model (see Ref. [39]), which stands as a wedge between the antiferromagnetic (AF) phase and the ordered spin ice (OSI) phase. The figure is a sketch of a cut in the exchange

- **Frustrated magnets Diffuse Scattering**

Practical volume now > 400 mm³ CN

2-3 orders and 3D q access needed CN

● Frustrated Magnets in field

PHYSICAL REVIEW B 88, 184428 (2013)

Magnetic structure in the spin liquid $\text{Tb}_2\text{Ti}_2\text{O}_7$ induced by a $[111]$ magnetic field:
Search for a magnetization plateau

A. P. Sazonov,^{1,2,3,*} A. Gukasov,³ H. B. Cao,^{4,3} P. Bonville,⁵ E. Ressouche,⁶ C. Decorse,⁷ and I. Mirebeau³

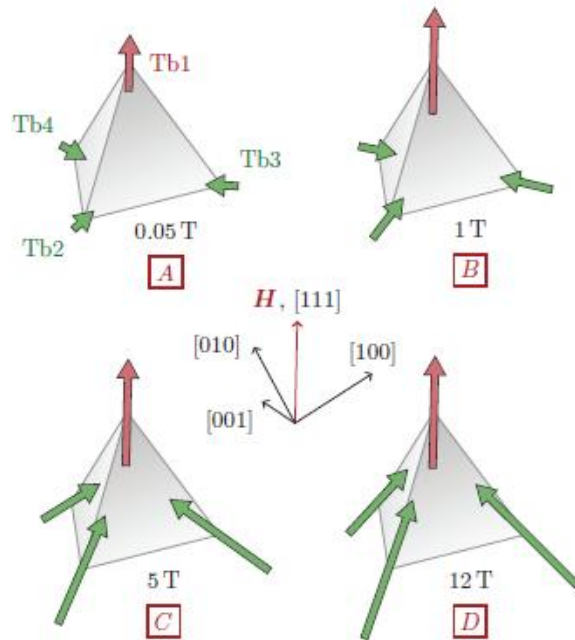


FIG. 4. (Color online) Field dependence of the Tb magnetic moments of $\text{Tb}_2\text{Ti}_2\text{O}_7$ at 300 mK under $H \parallel [111]$, for typical field values (cases A to D in Fig. 3). Only a single tetrahedron is shown for simplicity.

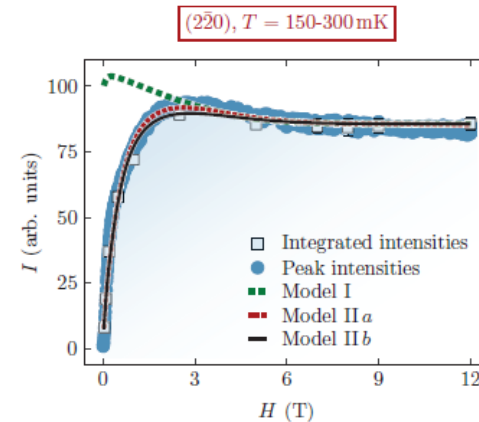


FIG. 10. (Color online) Field dependence of the $(2\bar{2}0)$ Bragg reflection under $H \parallel [111]$. The blue open squares correspond to the integrated intensities obtained with the data collections at 300 mK, and the blue closed circles are peak intensities measured during the field scans at 150–200 mK. Error bars are smaller than the symbol size if not given. The lines are mean-field calculations described in Sec. V. The green dashed line corresponds to Model I (no symmetry breaking). The red dotted and black solid lines are Model II *a* (quantum mixing with static Jahn-Teller effect) and Model II *b* (quantum mixing with dynamic Jahn-Teller effect), respectively. The two variants of the Model II yield the same result within less than 5% for all calculated Bragg peaks.

- **Frustrated magnets**

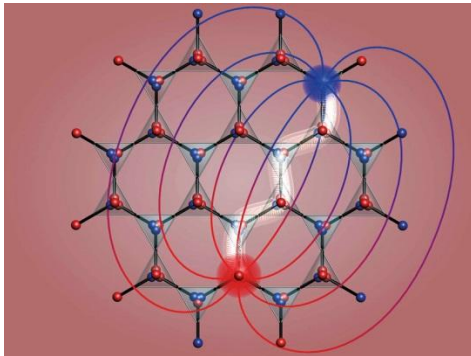
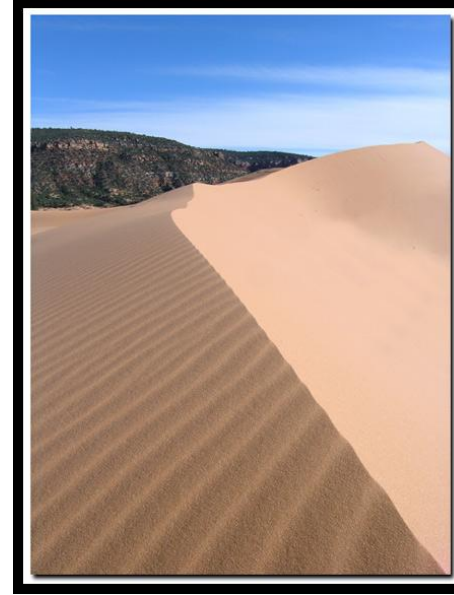
Magnetic Field , Multipolar interactions

Practical volume now > 10 mm³ HN

**High q_{\max} needed and data redundancy
for various corrections HN**

[1] W. Witczak-Krempa W. al. Annual Review of Cond. Matt. Phys., 5, 57, 2014

● Emergent Phenomena



SAZONOV, GUKASOV, MIREBEAU, AND BONVILLE

PHYSICAL REVIEW B **85**, 214420 (2012)

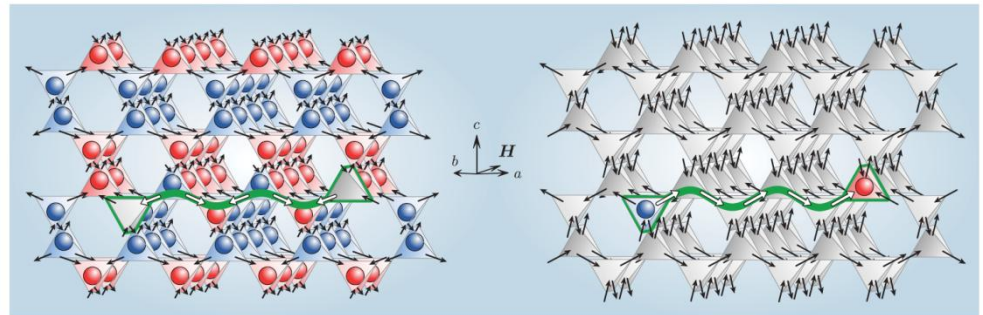
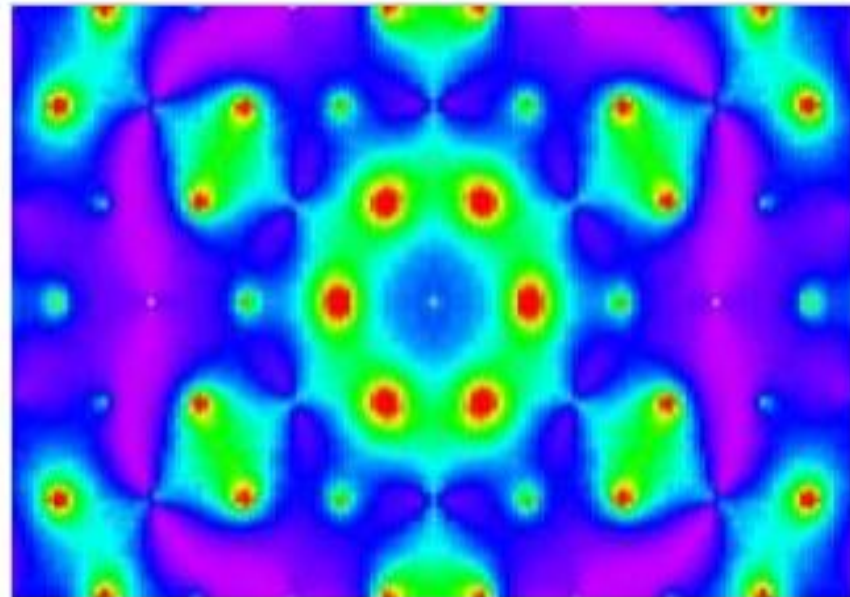
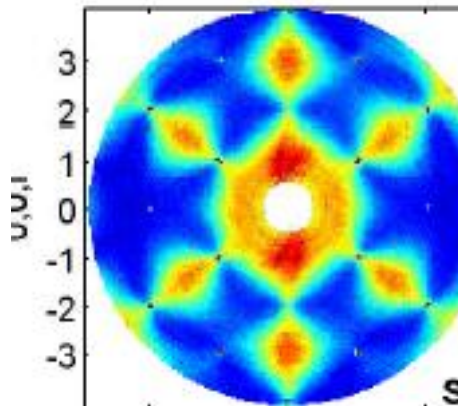


FIG. 5. (Color online) Left panel: Double-layered monopolar structure of $Tb_2Ti_2O_7$ with vacuum pair excitations. Right panel: Magnetically vacuum state of $Ho_2Ti_2O_7$ with monopole pair excitation.

Magnetic monopoles in spi

C. Castelnovo¹, R. Moessner^{1,2} & S. L. Sondhi³

● Emergent Phenomena



Dirac Strings as cosmic plasma filaments without attached dark matter components connecting galaxies together by magnetic currents to form the fractal filamentary web of the universe.

components connecting galaxies together by magnetic currents to form the fractal filamentary web of the universe.

$$\vec{m} = \overline{\chi} \vec{H}$$

$$\vec{F}_M(\vec{Q}) = \sum_k^{\text{atoms}} \overline{\chi}_k \vec{H} f_k(\vec{Q}) \exp(i\vec{Q} \cdot \vec{r}_k)$$

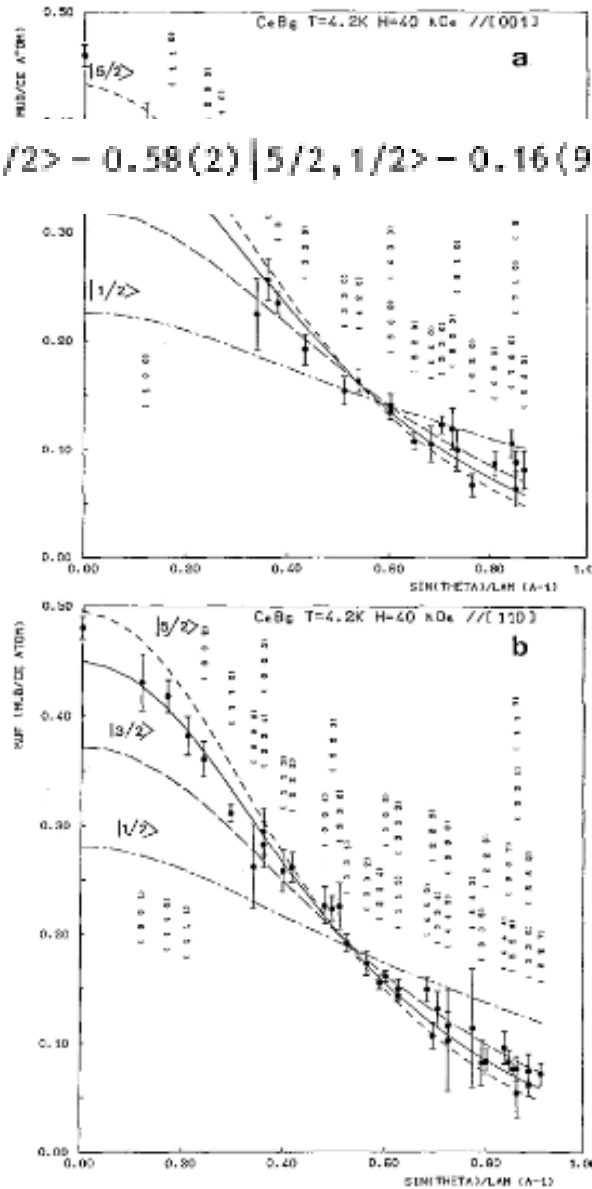
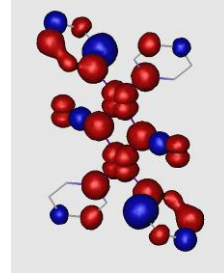


Figure 2 - Magnetic form factor of Ce^{3+} ion in CeB_6 . Experimental points correspond to measurements at $T = 4.2\text{ K}$ and $H^{\parallel} = 40\text{ kOe}$ parallel to the $[001]$ (a) and $[110]$ (b) direction. The calculated values for the dipole approximation (full line), a $|1/2\rangle$ (dash-dotted line), a $|3/2\rangle$ and a

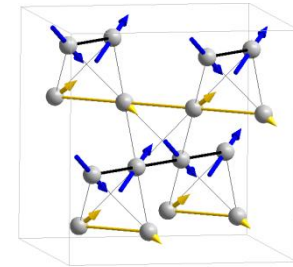
$$|\phi\rangle = 0.80(1) |5/2, 5/2\rangle - 0.58(2) |5/2, 1/2\rangle - 0.16(9) |5/2, -3/2\rangle$$

PND PROVIDES

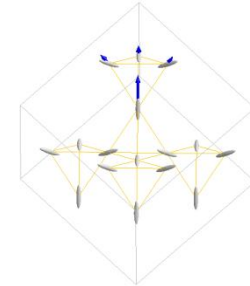
- Spin Densities



- Magnetic structure refinement



- Atomic Susceptibility Parameters



- Non-collinear Magnetization Densities ?